


12-2018

Assessing Biofiltration without Ozonation for Removal of Trihalomethane Precursors in Drinking Water at the Beaver Water District Drinking Water Treatment Plant

Sana Ajaz

University of Arkansas, Fayetteville

Follow this and additional works at: <https://scholarworks.uark.edu/etd>

 Part of the [Biological Engineering Commons](#), [Environmental Chemistry Commons](#), [Environmental Engineering Commons](#), [Environmental Health Commons](#), [Environmental Monitoring Commons](#), and the [Natural Resources Management and Policy Commons](#)

Recommended Citation

Ajaz, Sana, "Assessing Biofiltration without Ozonation for Removal of Trihalomethane Precursors in Drinking Water at the Beaver Water District Drinking Water Treatment Plant" (2018). *Theses and Dissertations*. 3111.
<https://scholarworks.uark.edu/etd/3111>

This Thesis is brought to you for free and open access by ScholarWorks@UARK. It has been accepted for inclusion in Theses and Dissertations by an authorized administrator of ScholarWorks@UARK. For more information, please contact scholar@uark.edu, ccmiddle@uark.edu.

Assessing Biofiltration without Ozonation for Removal of Trihalomethane Precursors in
Drinking Water at the Beaver Water District Drinking Water Treatment Plant

A thesis submitted in partial fulfillment
of the requirements for the degree of
Master of Science in Civil Engineering

by

Sana Ajaz
University of Engineering & Technology, Lahore
Bachelor of Science in Environmental Engineering, 2015

December 2018
University of Arkansas

This thesis is approved for recommendation to the Graduate Council.

Julian Fairey, Ph.D.
Thesis Director

Kieu Ngoc Le, Ph.D.
Committee Member

Wen Zhang, Ph.D.
Committee Member

Abstract

Biofiltration without pre-ozonation has the capability to remove natural organic matter (NOM) fractions that serve as precursors of disinfection byproducts (DBPs), which include the four regulated trihalomethanes (THMs) and dichloroacetonitrile (DCAN). Rapid small-scale column tests (RSSCTs) and Pilot Plant filters operated at empty-bed contact times (EBCTs) of 4, 8, and 16 minutes were used to evaluate the performance of nutrient-amended (free ammonia and phosphorus) biofiltration for THM and DCAN precursor removal, as measured using formation potential (FP) tests. NOM surrogates – which include dissolved organic carbon (DOC), specific ultraviolet absorbance ($SUVA_{254}$) and fluorescence-PARAFAC components – were measured weekly throughout the 30-week study to assess their suitability to track DBP precursor removal. RSSCTs containing DOC-exhausted granular activated carbon (GAC) removed up to 25% of the DOC with removal increasing ($\alpha=0.01$) with EBCT between 4 and 16 mins. During the 11-week period of active nitrification in the RSSCTs, average removals of total THMFP and DCANFP were 21% and 44%, respectively. However, statistically similar removals ($\alpha=0.01$) were observed at 8 and 16 mins EBCT, indicating that EBCTs in excess of 8 mins would not be helpful unless additional pretreatment steps such as pre-ozonation or a higher chlorine dioxide dose were added prior to the biofilters to increase the amount of biodegradable NOM. Relative to the RSSCTs, the Pilot filters achieved higher average removals of DOC, $SUVA_{254}$, TTHMFP and DCANFP because their GAC media was not exhausted with respect to DOC and thus NOM was sorbed by physical-chemical mechanisms. Weak linear correlations observed between NOM surrogates and TTHMFP ($R^2 < 0.27$) during the active nitrification period in the RSSCTs indicate that these surrogates are not useful for monitoring THM precursor removal in nutrient-enhanced biofilters and therefore DBPFP tests are required to assess biofiltration performance.

Acknowledgements

I would like to thank my advisor Dr. Julian Fairey and co-advisor Dr. Wen Zhang for giving me the opportunity to work on this exciting research project. It has been a challenging yet rewarding experience. I would also like to thank them for their counsel throughout the project, especially to Dr. Fairey for his diligent review of this document. I greatly appreciate the assistance provided by Bill Hagenburger and Danny Dearing at the Beaver Water District. I would also like to acknowledge the valuable insights and training provided by my colleague Thien Do during this project.

I am extremely grateful for the love and support I have received from my family and friends, especially my parents, throughout my stay in U.S. I would not have achieved this milestone without them. Finally, I must thank Shehroz for his unending love and support. He made this endeavor all the more worthwhile.

Table of Contents

1	Introduction and Motivation.....	1
2	Methods and Materials.....	5
2.1	Overview.....	5
2.2	Sample Site and Water Collection for Lab-Scale Testing.....	5
2.3	Reagent Preparation and Washing Procedures.....	6
2.4	Rapid Small-Scale Column Tests.....	7
2.5	Pilot scale testing.....	9
2.6	Water Quality Testing.....	10
2.7	Monochloramine Preparation.....	11
2.8	Dosing and Quenching.....	12
2.9	DBPFP Analyses.....	13
2.10	Statistical Analyses.....	14
3	Results and Discussion.....	15
3.1	Overall Treatment performance.....	15
3.2	Fluorescence PARAFAC analysis.....	19
3.3	Removal of DBP precursors.....	20
3.4	Correlations between PARAFAC components.....	26
3.5	Assessment of NOM Surrogates as DBP Precursors.....	26
3.6	Impact of nutrient supplementation.....	29
4	Conclusion and Future Work.....	31
5	References.....	33
6	Appendix.....	37

1 Introduction and Motivation

Chlorine is the most widely used drinking water disinfectant in the United States and worldwide. During chlorination, free chlorine (HOCl/OCl^-) reacts with natural organic matter (NOM) to form halogenated disinfection by-products (DBPs), such as trihalomethanes (THMs) (Rook 1974, Richardson et al. 2012) at concentrations up to several hundred micrograms per liter. Identification of THM precursor structures remains elusive due to the complicated mixture of organics within NOM, but general categories are well known and include aquatic humic substances, of which hydroxylated benzene structures within humic and fulvic acids are considered to be important in addition to algae and their metabolic products (Brezonik et al. 2011). Epidemiological evidence suggests chronic DBP exposures are associated with increased risks of kidney and colon cancers and adverse reproductive outcomes (Bull et al. 1991, Morris et al. 1992). The USEPA regulates four THMs – trichloromethane (TCM), dichlorobromomethane (DCBM), dibromochloromethane (DBCM), and tribromomethane (TBM) – in drinking water under the Stage 1 and 2 Disinfectants and Disinfection Byproducts (D/DBP) Rules at a Maximum Contaminant Level (MCL) of $80 \mu\text{g/L}$ for their summed mass-based concentrations. Other unregulated DBPs, such as haloacetonitriles (HANs) – which include dichloroacetonitrile (DCAN), trichloroacetonitrile (TCAN), bromochloroacetonitrile (BCAN), and dibromoacetonitrile (DBAN) – also form in many treated waters and have been shown to be more toxic than regulated THMs and haloacetic acids in *in vitro* bioassays (Muellner et al. 2007). However, curbing the formation of THMs and HANs in drinking water poses a major challenge for many drinking water treatment plants (DWTPs) across the United States, including the Beaver Water District (BWD) in Northwest Arkansas.

To curb THM formation, strategies have been developed to enhance NOM removal within the DWTP or switch to an alternative disinfectant such as monochloramine or chlorine dioxide. One

proven method for achieving enhanced NOM removal and, in turn, controlling DBP formation, is biofiltration. This is a multipurpose treatment process that can remove a wide range of dissolved organic carbon (DOC) and inorganic contaminants from water (Zhu et al. 2010). Biofiltration is achieved when the filters are fed with water containing little or no disinfectant which allows the development of an active biofilm on and within the filter media. Microorganisms in the biofilm can oxidize reduced inorganics such as free ammonia ($\text{NH}_4^+/\text{NH}_3$) and manganese (Mn^{2+}) (Kohl et al. 2012). Organics are removed by the microorganisms during biofiltration in two ways: (1) primary substrate utilization, in which a fraction of the NOM – namely, the so-called assimilable organic carbon (AOC) – is consumed as the carbon source during metabolism (Benner et al. 2013) and (2) co-metabolism, in which other organic compounds are biodegraded by bacteria using enzymes produced in primary substrate utilization (Zearley et al. 2012). Biofiltration leverages these metabolic processes to help produce biologically stable water and promote the degradation and removal of NOM fractions that serve as DBP precursors (Carlson et al. 1998, Liao et al. 2013). Granular activated carbon (GAC) has proven to be an effective filtration media for biofiltration as it supports microbial growth within its internal pore structure and its exterior particle surfaces. This is primarily attributed to the structural characteristics of GAC such as high porosity and surface roughness (Luo et al. 2014). One added advantage of using GAC for biofiltration is that microorganisms are able to continuously degrade some sorbed organics and replenish active sorption sites within the GAC (Cheremisinoff et al. 1978, Rice et al. 1982). This process, referred to as biological regeneration, increases the service life of GAC, and can potentially be sustained indefinitely. However, in practice, ca. 5-10% of the GAC is replaced per year due to losses from filter backwashing and GAC particle friability.

Other than filter media type, pretreatment affects the efficacy of biofiltration for removing DBP precursors. Ozonation often precedes biofiltration for enhanced NOM removal (McKie et al. 2015, Liu et al. 2017) by transforming recalcitrant high molecular weight NOM to biodegradable fractions (Basu et al. 2016) that are more readily utilized by the microorganisms. While it has been demonstrated that ozone-biofiltration provides enhanced removal of NOM (Price et al. 1993, Selbes et al. 2017), the addition of ozonation at a DWTP entails significant capital and operational costs. This has compelled the water industry to assess biofiltration without pretreatment for the removal of NOM. Studies have shown biofiltration without pretreatment to be effective in removing regulated DBP precursors (Price et al. 1993, Wang et al. 1995). Fu et al. (2017) reported a 19% reduction in total THM formation potential (TTHMFP) and a 26% reduction in haloacetic acid (HAA) FP but negative removal (-9%) or, in actuality, precursor production of four haloacetonitriles (DCAN, BCAN, TCAN and DBAN) in pilot scale GAC biofilters aided with nutrients and operated at an empty-bed contact time (EBCT) of 15 mins. This production of haloacetonitriles was likely due to release of soluble microbial products by the microorganisms in the biofilter. Another pilot scale biofiltration study without pre-ozonation showed ~20% and ~12% removal of TTHMFP and HAAFP, respectively, using an EBCT of 11 mins (Azzeh et al. 2015).

The objective of this study is to determine the extent of THM and HAN precursor removal that can be achieved in nutrient enhanced nitrifying biofilters in the absence of ozone pretreatment. Bench and pilot scale studies were completed using biologically active GAC filters to evaluate removal of THM and HAN precursors and seasonal variations in settled water from the BWD. Supplemental nutrients (free ammonia and phosphate) were added for an 11-week period to promote growth of nitrifying microorganisms in the biofilters. While nitrifiers are autotrophs (i.e., they use carbon dioxide as their carbon source), their activity can be monitored by measurement

of inorganic nitrogen species and it has been demonstrated that their presence promotes the degradation of THMs through co-metabolism (Aziz et al. 1999, Wahman et al. 2005). NOM surrogates including UV_{254} , DOC, $SUVA_{254}$, and fluorescence-based metrics were monitored throughout the 30-week study. Four THMs and four HANs were measured for 19 weeks following a modified DBP formation potential (DBPFP) test with monochloramine (Do et al. 2015). Lastly, correlations were sought between DBP precursor removal and the various spectroscopic metrics, the strength of which proved to be adversely impacted during the active nitrification period.

2 Methods and Materials

2.1 Overview

This chapter covers the methodical details of sampling, reagent preparation, and water quality testing procedures used in this study. Operational parameters and modifications for the pilot plant and lab-scale setups are detailed. The water quality parameters analyzed were dissolved organic carbon (DOC), pH, free ammonia, UV₂₅₄, fluorescence excitation-emission matrices (EEMs), and major anions in drinking water. The approach used to assess the disinfection byproduct formation potential (DBPFP) is detailed, including disinfectant type and dosing, incubation conditions, residual quenching, and DBP extraction and measurement using a Gas Chromatogram (GC) equipped with an electron capture detector (ECD).

2.2 Sample Site and Water Collection for Lab-Scale Testing

The Beaver Water District (BWD) drinking water treatment plant (DWTP) located in Lowell, AR treats Beaver Lake water and distributes drinking water to the four major cities in Northwest Arkansas. When the DWTP was first constructed in 1966, it consisted of the JM Steele Plant which had a treatment capacity of 10 MGD. The facility was expanded over the years to increase its treatment capacity to accommodate the population growth of Northwest Arkansas. Presently, the DWTP consists of the Steele and Croxton Plants that run as two separate trains having different structural designs but follow similar treatment regimes. The combined daily capacity of the DWTP is now 140 MGD and the average daily demand is 55.1 MGD with a peak demand of 90 MGD in the summer months. BWD sells drinking water to customer cities of Fayetteville, Springdale, Rogers, and Bentonville for use and subsequent resale to 14 surrounding municipalities. According to BWD production data, in September 2016 BWD supplied drinking water to approximately 330,000 people in Northwest Arkansas.

The treatment regime at the BWD DWTP includes primary disinfection, coagulation, flocculation, settling, filtration, and secondary disinfection. At the intake, raw water is amended with 1 mg/L chlorine dioxide and 0.65 mg/L gaseous chlorine (45 kg/day). Alum (30 mg/L) is added as primary coagulant at the flash mix basin along with ferrous sulfate (6.5 mg/L) and cationic polymer (1 mg/L) to promote floc growth and improve settling. The ferrous sulfate is added to chemically reduce the chlorite formed from the reduction chlorine dioxide; in doing so, the ferrous iron is oxidized to ferric iron, a trivalent cation that acts as a secondary coagulant. Anionic/nonionic polymer (0.15 mg/L) is added at the second stage of flocculation to assist with the settling process. Free chlorine (1.5 mg/L) is added as secondary disinfectant to the finished water prior to the entry point to the distribution system.

For the lab-scale setup, approximately 70 L of water from settling basins of the full-scale BWD DWTP was collected weekly between March and October, 2018 and used as feedwater for lab-scale columns at the University of Arkansas. The settled water collected at the plant was transported to the lab in pre-cleaned 9 L HDPE carboys with screw top plastic lids. The carboys were stored in at 4°C in a cold room until use. Before using as feedwater for the columns, the water was brought to room temperature.

2.3 Reagent Preparation and Washing Procedures

All stock solutions, dilutions, and blanks were prepared using Milli-Q water (18.2 MΩ-cm) generated from Millipore Integral 3 Milli-Q water system (Billerica, MA). Chemicals used for the experiments were ACS grade. All samples were filtered using 0.45 μm polyethersulfone membrane syringe filters which were pre-rinsed with 300 mL of Milli-Q water prior to use. Filtered samples were used for all analysis except for free ammonia test as its measurement is not impacted by particulates.

The washing procedure for glassware began with soaking each item in a tap water bath containing Alconox detergent. After thorough scrubbing, all the glassware was rinsed three times with tap water, deionized (DI) water, and finally with Milli-Q water. Amber glassware and the glassware used for analyses with organic solvents was baked at 400 °C in a muffle furnace for at least 2 hours. Other glassware was washed and rinsed according to the aforementioned procedure but dried in a desiccator oven at 45 °C for at least 3 hours. PTFE lined lids, plastic ware, and precision glassware were washed and rinsed the same way followed by air drying. PTFE lined lids were triple rinsed with Acetone before being air-dried.

2.4 Rapid Small-Scale Column Tests

The laboratory setup for the rapid small-scale column tests (RSSCTs) consisted of a 50 L feedwater tank, a multichannel peristaltic pump, and four 1-cm inner diameter glass columns. The setup was modified on July 24th, 2018 to eliminate the need for adding nutrients to the feedwater tank. For this purpose, a custom-made mixing jug, a magnetic stirrer plate, and a syringe pump was introduced to amend the feedwater with nutrients immediately prior to the columns (see Figure 2-1). The columns were operated as two sets (A and B) in parallel with each set consisting of two columns in series. An inline filter (Whatman POLYCAP PES – 0.45 µm) was placed in the flowpath following the feedwater tank to prevent larger particles from entering the columns and causing pressure build-up. The packed-bed depth in each column was adjusted using plungers at both ends and the GAC media was held in place using glass wool as shown in Figure 2-1 (right-side photo).



Figure 2-1. Photographs of packed-bed columns. The left-side photo shows lab-scale RSSCT setup including a feedwater tank, inline filter, peristaltic pumps, mixing jug, stirrer, syringe pump, and glass columns filled with GAC. The right-side photo shows glass columns filled with GAC in a packed-bed set using plungers and glass wool.

The GAC used in the RSSCTs was 40×60 US Mesh Size (geometric mean, $d_{sc} = 0.33$ mm). A flowrate of 1.9 mL/min was maintained through the columns which equates to a hydraulic loading rate (V_{sc}) of 2.4 cm/min for the columns which have a cross-sectional area, $A = 0.785$ cm². The EBCTs maintained in column Sets A and B were 16 and 8 mins, respectively. Table 2-1 shows the operational parameters of the RSSCTs.

Table 2-1. Operational parameters for RSSCTs

Filter Train	Column Diameter (cm)	GAC Depth (cm)	Flowrate (mL/min)	EBCT (mins)	Reynolds Number (unitless)
Set A: A1 & A2	1.0	38	1.9	16	0.37
Set B: B1 & B2	1.0	19	1.9	8	0.37

In Table 2-1, the Reynolds Number was calculated using Equation 1, as follows:

$$Re = \frac{d * V_{sc}}{\epsilon * \nu} \quad (\text{Equation 1})$$

where, the geometric mean, d , of the GAC particle diameter for 40×60 US Mesh size particles is 0.33 mm, the hydraulic loading rate (HLR) of the column, $V_{sc} = 2.4$ cm/min, the porosity of the GAC bed, $\epsilon = 0.4$ (estimated), and the kinematic viscosity of water at room temperature (25°C), $\nu = 8.9 \times 10^{-7}$ m²/s. For adsorption analysis using RSSCTs, it is recommended to keep Reynold's (Re) number greater than or equal to 0.50 (Chowdhury 2013). However, as shown in Table 2-1, the Re number in this study was 0.37, to provide more EBCT for biofiltration and maintain a suitable pressure drop throughout the RSSCTs. A lower Re number as a result of low flowrate may produce an external (or film) mass transfer limitation of the substrate diffusing from bulk liquid to the biofilm surface (Beyenal et al. 2002) which may adversely impact removal. However, studies have also shown that in biofiltration, removal of organic compounds is more dependent on EBCT than filtration rate (Servais et al. 1994).

2.5 Pilot scale testing

During the period of operation of the lab-scale study, pilot-scale testing was carried out at the pilot facility located onsite at BWD plant. The pilot plant includes two identical parallel treatment trains, each representing the scaled down version of Steele and Croxton plants. The pilot trains received raw water coming from the intake and passed through the flash mixer, flocculation basins, settling basins and filters before ending up in the clear-well.

For the purpose of this biofiltration study, parallel filters of Train 2 at the pilot plant were utilized with modifications. An additional HDPE pipe (diameter = 5 cm, length = ca. 137 m) was laid to transport settled water directly from the full-scale settling tanks to an equalization basin within the pilot plant. The tank served as the source of settled water to the pilot filters. Two filters, one Croxton and the other Steele, were filled with fresh GAC media (Calgon F-400-M) in May 2018. Table 2-2 shows media depth, flowrates, and EBCT maintained through Steele and Croxton Filters.

Table 2-2. Operational parameters for the pilot plant filters at the BWD

Filter	Column Diameter (cm)	Media Depth (cm)	Flowrate (L/min)	EBCT (mins)
Steele	20	152	3.00	16
Croxton	20	122	4.92	8

Throughout the pilot study, filter influent was supplemented with phosphate (0.1 mg/L as P) to enhance biological growth within the filters. Ammonium (1 mg/L as N) was also added beginning in September 2018 to induce nitrification in biofilters, similar to the lab-scale filters. The pilot filters were backwashed weekly in two steps, first through air scouring and then flushing with non-chlorinated filtered water. Backwash water was sourced from a large holding tank in the pilot plant that stored filtered water. Samples were collected before each backwash i.e., after a filtration cycle of ~144 hrs or 6 days.

2.6 Water Quality Testing

The following water quality parameters were measured for both lab and pilot-scale study samples: DOC, pH, free ammonia, UV_{254} , fluorescence EEMs, and anions which included nitrate, nitrite, bromide, and phosphate. DOC was measured with a Sievers 5310C Portable TOC Analyzer (Sievers, Boulder, CO). Sample pH was measured with an Orion 8272 electrode (Thermo Orion, Waltham, MA). The electrode was calibrated weekly with pH standards of 4, 7 and 10. Free ammonia was measured using ammonia electrode (Thermo Orion 9512, Beverly, MA) connected to an Accumet XL60 meter. Precisely, 0.5 mL of alkaline reagent (Orion 951011) was added to 50 mL of sample to measure the total free ammonia. The electrode was calibrated before each use with free ammonia standards of 0.01, 0.1, and 1 mg/L-N, prepared using ammonium chloride in

Milli-Q water. UV_{254} was measured on a spectrophotometer using 5 cm quartz cuvette. The cuvette was triple rinsed with Milli-Q water after scanning each sample.

Fluorescence measurements were done using an Agilent 1200 Series fluorescence detector. Duplicates were run for each sample and the syringe used for filling the cuvette was triple rinsed between each sample with secondary-clean and clean Milli-Q water. All EEM scans were corrected for first- and second-order Rayleigh and Raman water scattering using a MATLAB® Cleanscan program developed by Zepp et al., (Zepp et al. 2004). The resulting 426 EEMs were subjected to PARAFAC analysis which established a 3-component model. The model was validated using split halves analysis after removal of five outliers. Further details on EEM collection, scatter correction and PARAFAC analyses can be found in Pifer et al. (2011).

A Metrohm Professional Ion Chromatograph, Model 850.3040 (Riverview, FL) was used to analyze anions. A 3.6 mM sodium bicarbonate solution was used as an eluent. For each new batch of eluent or after every 120 samples, a standard curve was run using calibration standards at 0.1, 0.2, 0.5, 1.0, 5.0, 10.0, 25.0 and 50.0 mg/L. These standards were prepared from Metrohm stock solution (REAIC1035) containing fluoride, chloride, nitrite, bromide, nitrate, phosphate, and sulfate. One check standard at 1.0 mg/L was run with each batch every 12 samples. All checks were found to be within 1% of the standard.

2.7 Monochloramine Preparation

Monochloramine stock solution of ca. 7,000 mg/L- Cl_2 was prepared fresh before dosing to assess DBP precursor removal in the lab- and pilot-scale filters. The concentration of monochloramine was kept high to minimize the dilution error. The maximum dosing volume was maintained less than 5% of the sample volume. For monochloramine preparation, chilled sodium hypochlorite solution (ca. 5°C) was added with a glass pipette drop-wise to a rapidly mixing (ca. 650 rpm) 0.4

M ammonium chloride solution. The concentration of both reagents were such as to achieve a Cl₂:N mass ratio of 4.55:1 (Method 10200 – Hach Company). When preparing ammonium chloride solution, it was buffered with sodium bicarbonate such as to yield a 20 mM NaHCO₃ monochloramine stock solution, and adjusted to pH 8.3. After all the sodium hypochlorite was added to the ammonium chloride solution, the monochloramine stock was left to mix at ca. 300 rpm for 10 minutes. A 250- and 200-fold dilution of the stock were prepared and measured using a UV spectrophotometer (Shimadzu UV-Vis 2450) at a wavelength range of 245-295 nm. This absorbance range corresponds to concentrations of monochloramine and dichloramine (Schreiber et al. 2005) which were then determined using Equations 2 and 3, as follows:

$$A_{245} = \epsilon_{NH_2Cl,245} * C_{NH_2Cl} * l + \epsilon_{NHCl_2,245} * C_{NHCl_2} * l \quad (\text{Equation 2})$$

$$A_{295} = \epsilon_{NH_2Cl,295} * C_{NH_2Cl} * l + \epsilon_{NHCl_2,295} * C_{NHCl_2} * l \quad (\text{Equation 3})$$

In Equations 2 and 3, A is the absorbance reading at a particular wavelength as measured by the UV spectrometer, ϵ is the molar extinction coefficient (M⁻¹cm⁻¹) at a specified wavelength ($\epsilon_{NH_2Cl,245} = 445$, $\epsilon_{NHCl_2,245} = 208$, $\epsilon_{NH_2Cl,295} = 14$, $\epsilon_{NHCl_2,295} = 267$), C is the molar concentration of chloramine species, and l = cuvette path length (1 cm).

2.8 Dosing and Quenching

Before dosing samples from the RSSCTs or pilot plant filters with monochloramine to assess DBPFP, they were adjusted to pH 7 by adding a bicarbonate buffer followed by the addition of hydrochloric acid (Do et al. 2015). The volume of these additions was kept lower than 5% of the sample volume. When dosed with monochloramine, all samples were mixed well and made headspace-free in amber bottles capped with PTFE-lined lids. All sample bottles were shielded from light and kept at room temperature (25 ± 2 °C) for 7 days. On the day of extraction, 30 mL

of each sample was transferred to a 40 mL vial, each containing 400 mg of dry quenching mix. This was done to ensure that all DBP formation reactions have stopped. The quenching mix had a weight ratio of 1.8-to-1-to-39 (0.9 g ascorbic acid, 1 g KH_2PO_4 , and 39 g Na_2HPO_4).

2.9 DBPFP Analyses

Quenched samples were extracted immediately into n-pentane following EPA Method 551.1 with modifications (Pifer et al. 2012). DBPFP for THMs and DHANs was quantified using GC-ECD (Shimadzu 2010). Total THMs included trichloromethane (TCM), dichlorobromomethane (DCBM), dibromochloromethane (DBCM), and tribromomethane (TBM). Total HANs were comprised of dichloroacetonitrile (DCAN), trichloroacetonitrile (TCAN), bromochloroacetonitrile (BCAN), and dibromoacetonitrile (DBAN). A seven-point standard curve ranging from 0.1-20 $\mu\text{g/L}$ of each DBP was established to quantify THMs and HANs as well as blanks and check standards. This range was selected to encompass the DBPFP of the samples. Blanks and check standards were run after every eighteenth injection. As per EPA Method 551.1, all checks were within $\pm 25\%$ of the standard while 90% of them were within $\pm 20\%$. Table 2-3 shows Method Detection Limit (MDL) for each DBP analyzed. These MDLs were determined by running seven replicates for each sample and determining the standard deviation among the seven replicates. Equation 4 was used to determine the MDL for each DBP:

$$MDL = \text{standard deviation} \times t_{\text{value}} \quad (\text{Equation 4})$$

Table 2-3. Method Detection Limit (MDL) for each disinfection byproduct analyzed

Disinfection byproduct	Abbreviation	MDL ($\mu\text{g/L}$)
Trichloromethane	TCM	0.30
Dichlorobromomethane	DCBM	0.06
Dibromochloromethane	DBCM	0.07
Tribromomethane	TBM	0.05
Trichloroacetonitrile	TCAN	0.36
Dichloroacetonitrile	DCAN	0.05
Dibromoacetonitrile	DBAN	0.05
Bromochloroacetonitrile	BCAN	0.06

The t-value for seven replicates and six degrees of freedom is 3.143. The MDLs ranged from 0.05-0.36 $\mu\text{g/L}$ for the THMs and DHANs and were used as the threshold reporting limits for each analyte.

2.10 Statistical Analyses

Comparisons of percent removals in the RSSCTs and Pilot filters for DOC, SUVA_{254} , TTHMFP, and DCANFP were made using Tukey’s paired comparison method (Brown et al. 2002) using the studentized range statistic for two-sided comparisons for a joint 99% confidence interval ($\alpha=0.01$). This alpha value was selected such that differences are very significant, despite that an alpha of 0.01 corresponds to a “false-alarm” probability of at least 11% (Nuzzo 2014). This means that comparisons determined to be statistically different at the $\alpha=0.01$ level have approximately a 9 in 10 chance of being a result of a true effect. By comparison, should an alpha of 0.05 been selected, as is most common in the environmental engineering field, this “false-alarm” probability is at least 29% and only a 7 in 10 chance of a statistically different result being a true effect.

3 Results and Discussion

3.1 Overall Treatment performance

The NOM surrogates measured include UV_{254} , DOC, and fluorescence-based metrics and were monitored for both the RSSCTs and Pilot filters throughout the study period. $SUVA_{254}$ was calculated by dividing UV_{254} by the DOC. Figures 3-1 and 3-2 show the DOC and $SUVA_{254}$ profiles from the RSSCTs and Pilot filters, respectively. Overall, the influent DOC varied between 1.2-2.5 mg/L-C and $SUVA_{254}$ between 0.7-2.8 L/mg-m, indicating that the water had low organic carbon content, an expected result for the ClO_2 -treated and coagulated-settled BWD water. Additionally, removal of DOC and $SUVA_{254}$ occurred in the RSSCTs and Pilot filters (Figures 3-1 and 3-2 and Table 3-1). For the RSSCTs containing GAC exhausted with respect to DOC, the average DOC removal increased ($\alpha = 0.01$) from the Influent to A1, A1 to A2, and the Influent to B2, indicating more removal with increasing EBCT between 4 and 16 mins; further, for an EBCT of 8 min (i.e., A1 and B2), there was no difference ($\alpha = 0.01$) in average DOC removals. Similar average removals and trends for $SUVA_{254}$ were observed (Table 3-1). In the Pilot filters, higher average DOC removal ($\alpha = 0.01$) was observed in Steele (66%) than in Croxton (33%) for EBCTs of 16- and 8 mins, respectively. This is expected as the GAC in Pilot filters was not exhausted with respect to DOC and the total bed volumes fed were less than half of the RSSCTs (Figures 3-1 and 3-2). Comparison with biofiltration studies without pre-ozonation indicates that the DOC removal from the RSSCTs was comparable in some cases and lower than others. Akcay et al. (2016) observed 50% and 65% DOC removal for EBCTs of 15- and 30 mins, respectively. Fu et al. (2017) reported > 24% removal of DOC and > 44% removal of $SUVA_{254}$ in pilot biofilters operated at an EBCT of 15 mins with nutrient-amended source water. Notably, the effluent $SUVA_{254}$ was higher than the influent in both the Steele and Croxton filters during the active nitrification period (shaded

region in Figure 3-2D) despite DOC removal (Figure 3-2B), which indicates a positive interference in the UV₂₅₄ measurement. This is due to the formation of nitrate from biological ammonia oxidation and is further explained in Section 3.6.

Table 3-1. Percent Removal of DOC and SUVA₂₅₄ in the RSSCTs and Pilot filters

Column	EBCT (minutes)	Average % Removal ± 99% Confidence Interval	
		SUVA ₂₅₄	DOC
A1	8	16 ± 7 ^{i(≈)}	17 ± 7 ^{i(≈)}
A2	16	25 ± 7 ⁱⁱ	25 ± 7 ⁱⁱ
B1	4	9 ± 7 ⁱ	5 ± 7
B2	8	18 ± 7 ⁱⁱ	16 ± 7 ⁱ
Steele	16	31 ⁱ	66 ⁱ
Croxton	8	12 ⁱ	33 ⁱ

ⁱsignificantly different from influent at $\alpha=0.01$

ⁱⁱsignificantly different from influent and A1 or B1 at $\alpha=0.01$

^(≈)not significantly different from B2 at $\alpha=0.01$

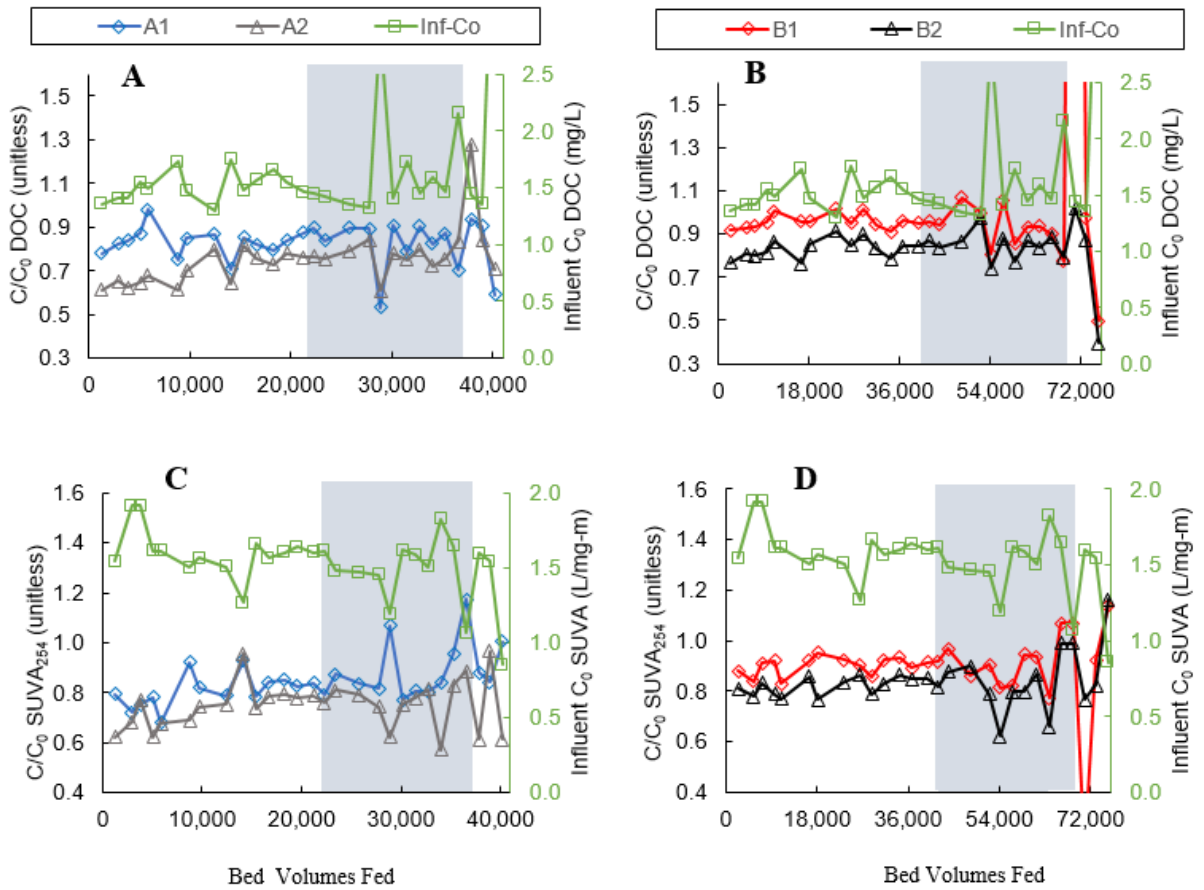


Figure 3-1. Influent-normalized profiles (C/C_0) in the RSSCTs for DOC (A and B) and $SUVA_{254}$ (C and D). Influent concentration (C_0) profiles are represented on the secondary y-axis. The shaded area represents the period for which the influent was supplemented with free ammonia at 1 mg/L-N.

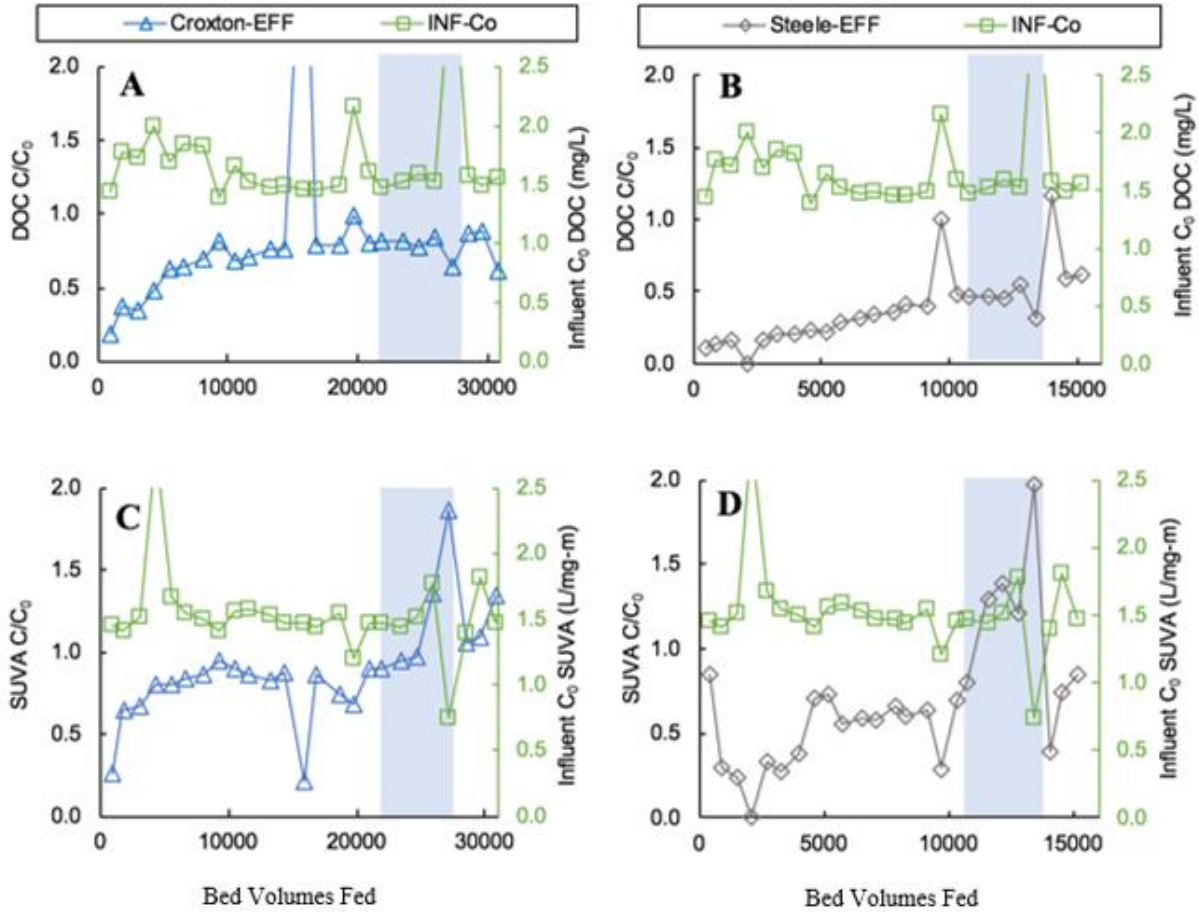


Figure 3-2. Influent-normalized profiles (C/C_0) in the Pilot filters (Steele and Croxton) for DOC (A and B) and $SUVA_{254}$ (C and D). Influent concentration (C_0) profiles are represented on the secondary y-axis. The shaded area represents the period for which the influent was supplemented with free ammonia at 1 mg/L-N.

3.2 Fluorescence PARAFAC analysis

Fluorescence indices determined from EEMs were obtained for both the RSSCTs and the Pilot filters. A total of 426 EEMs were subjected to PARAFAC analysis which resulted in a validated 3-component model following removal of five outliers. Excitation and emission peak values for the three components and their fluorophore identification are presented in Table 3-2 and shown in Figure A-1. PARAFAC components are generally characterized as humic-like, fulvic-like, or protein-like based on the location of their excitation-emission maxima. Component 1 (C1) appears to be fulvic-like fluorophores based on its excitation and emission maxima of 325 nm and 420 nm, respectively (Santín et al. 2009, Pifer et al. 2014). Component 2 (C2) has an excitation and emission maxima of 370 nm and 445 nm, respectively, and can be ascribed to humic-like fluorophores as suggested by Santín et al. (2009) and Coble (1996). Excitation and emission maxima for Component 3 (C3, 287 nm and 355 nm, respectively) most closely resemble fluorophores of amino acids (either free or protein-bound) (Baghoth et al. 2011). Correlations between PARAFAC components and DBPFP are detailed in Section 3.5.

Table 3-2. Excitation/Emission Maxima and Identification of the Fluorescence PARAFAC Components

Component number	Excitation maxima (nm)	Emission maxima (nm)	Identification	References
C1	235 (325)	420	Fulvic-like	Santín et al. (2009) Pifer et al. (2014)
C2	370 (266)	445	Humic-like	Santín et al. (2009) Coble (1996)
C3	230 (287)	355	Protein-like	Baghoth et al. (2011)

Values in parentheses are secondary excitation maxima

3.3 Removal of DBP precursors

NOM and particularly its dissolved fractions that react with chlorine-based disinfectants have demonstrated potential to form DBPs in raw and treated drinking water (Gopal et al. 2007, Richardson et al. 2012). DBPs formed in ClO₂-treated and coagulated-settled BWD water and biofilter effluent water from the RSSCTs and Pilot filters are presented as influent-normalized profiles in Figures 3-3 through 3-6. Overall, influent TTHMFP (Figure 3-3 and 3-4) ranged from 8-16 µg/L and the DCANFP (Figure 3-5 and 3-6) ranged from 0.6-2.5 µg/L. DCAN was the only haloacetonitrile detected in samples. The relatively low formation potential of the influent water can be attributed to the preceding treatment (ClO₂ oxidation and coagulation-settling) at BWD and to the alternative method used for assessing DBP precursor removal that utilizes a monochloramine dose of 250 mg/L-Cl₂ instead of targeting a free chlorine residual between 3-5 mg/L-Cl₂ (Do et al. 2015). Differences (0.8-27%) observed between the influent DBPFPs in the Pilot filters and RSSCTs could be because the settled water collected at BWD was stored in a cold room at 4 °C for up to one week before being utilized in the RSSCTs.

Biofiltration showed removal of TTHM and DCAN precursors in both the RSSCTs and Pilot filters (Figures 3-3 to 3-6) that generally increased with EBCT and was sustained throughout the active period of nitrification. For TTHM and DCAN precursors in the RSSCTs, Table 3-3 shows no statistically significant removal ($\alpha = 0.01$) in B1 (EBCT = 4 mins), but removal occurred in A1 (EBCT = 8 mins) to a similar extent as A2 (EBCT = 16 mins) and B2 (EBCT = 8 mins). The lack of statistically significant ($\alpha = 0.01$) increased removal from an EBCT of 8- to 16 mins suggests that additional EBCT would not be helpful, likely because the biodegradable NOM fraction was metabolized within the initial 8 min EBCT. Additional pre-treatment – such as ozonation or perhaps a higher chlorine dioxide dose – could be helpful in producing additional biodegradable

NOM that could subsequently be removed using additional EBCT. However, in the Pilot filters, removal of TTHMFP and DCANFP are higher in Steele (EBCT = 16 mins) compared to Croxton (EBCT = 8 mins) but these filters were removing DBP precursors by physical-chemical sorption in addition to biofiltration. Greater fractional removal of DCANFP as compared to TTHMFP for the RSSCTs and Pilot filters (Table 3-3) is similar to what Liu et al. (2017) reported based on biofiltration without pre-ozonation. Further, the extent of removal of TTHM precursors in the RSSCTs with exhausted GAC is similar to other biofiltration studies performed in the absence of pre-ozonation (Price et al. 1993, Wang et al. 1995, Liu et al. 2017). Fu et al. (2017) reported 19% reduction in TTHMFP for pilot scale GAC biofilters amended with nutrients at an EBCT of 15 mins. These conditions are similar to the pilot plant study in this work, however, greater removal of TTHMFP was observed in our case is most likely due to greater adsorption capacity of the relatively new GAC media in the pilot filters. The impact of nutrient addition on DBPFP removal is explained in Section 3.6.

Table 3-3. Percent Removal of TTHMFP and DCANFP in the RSSCTs and Pilot filters during the Period of Active Nitrification

Column	EBCT	% Removal ± 99% Confidence Interval	
		TTHMFP	DCANFP
A1	8	13 ± 10 ^{i(≈)}	31 ± 16 ^{i(≈)}
A2	16	21 ± 10 ⁱ	44 ± 16 ⁱ
B1	4	3 ± 10	15 ± 16
B2	8	15 ± 10 ⁱ	35 ± 16 ⁱ
Steele	16	46 ⁱ	60 ⁱ
Croxton	8	19 ⁱ	29 ⁱ

ⁱsignificantly different from influent at $\alpha=0.01$

ⁱⁱsignificantly different from influent and A1 or B1 at $\alpha=0.01$

^(≈)not significantly different from B2 at $\alpha=0.01$

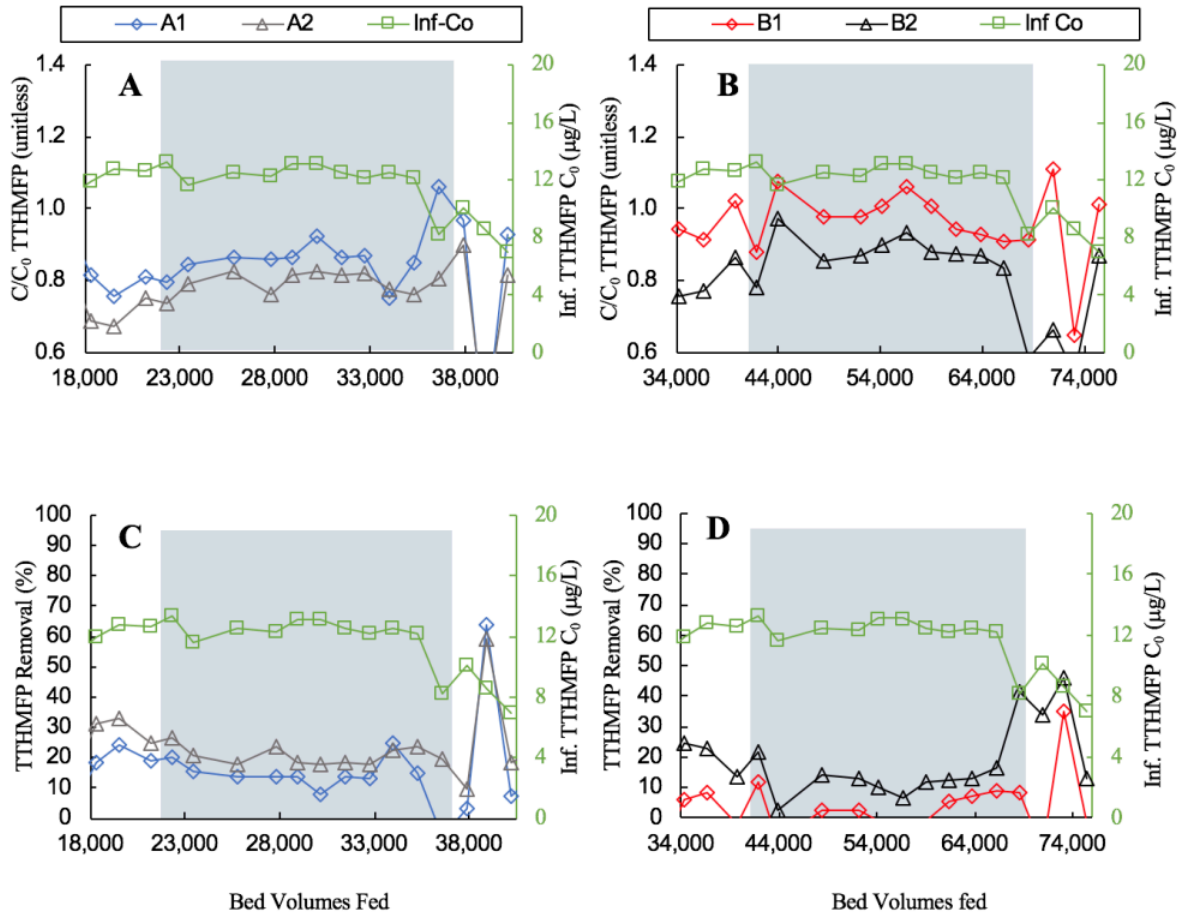


Figure 3-3. Influent-normalized profiles (C/C_0) in the RSSCTs for TTHMs (A & B) and % TTHMFP removal (C & D). Influent concentration (C_0) shown on the secondary y-axis. The shaded area represents the duration for which the influent was supplemented with free ammonia at 1 mg/L-N. The RSSCTs were run in parallel with each set consisting of two columns in series represented as A1, A2, B1 and B2. See text for additional details.

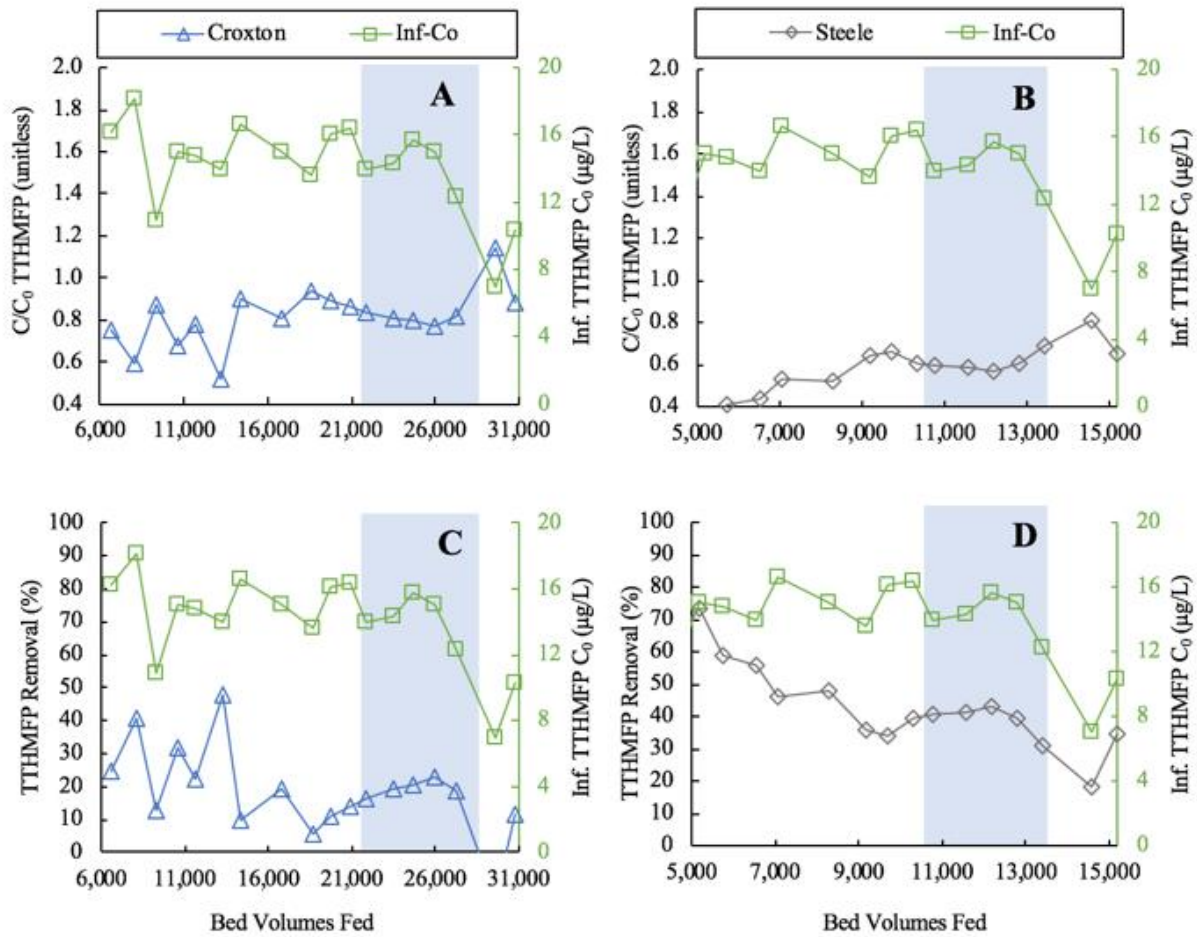


Figure 3-4. Influent-normalized (C/C_0) profiles in the Pilot filters for TTHMs (A & B) and % TTHMFP removal (C & D). Influent concentration (C_0) is shown on the secondary y-axis. The shaded area represents the duration for which the influent was supplemented with free ammonia at 1 mg/L-N.

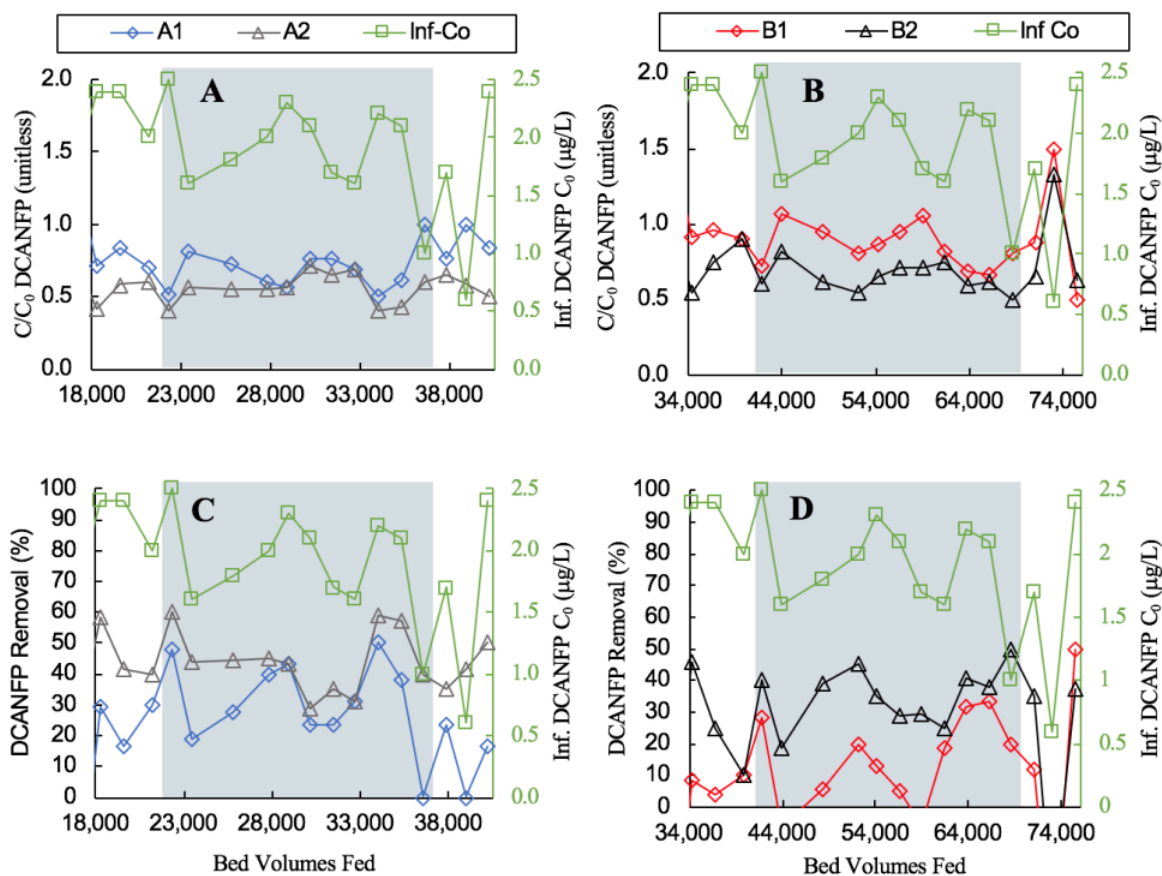


Figure 3-5. Influent-normalized (C/C_0) profiles in the RSSCTs for DCAN (A & B) and % DCANFP removal (C & D). Influent concentration (C_0) is shown on the secondary y-axis. The shaded area represents the duration for which the influent was supplemented with free ammonia at 1 mg/L-N. The two column sets (A & B) were run in parallel with each set consisting of two columns in series represented as A1, A2, B1 and B2. See text for additional details.

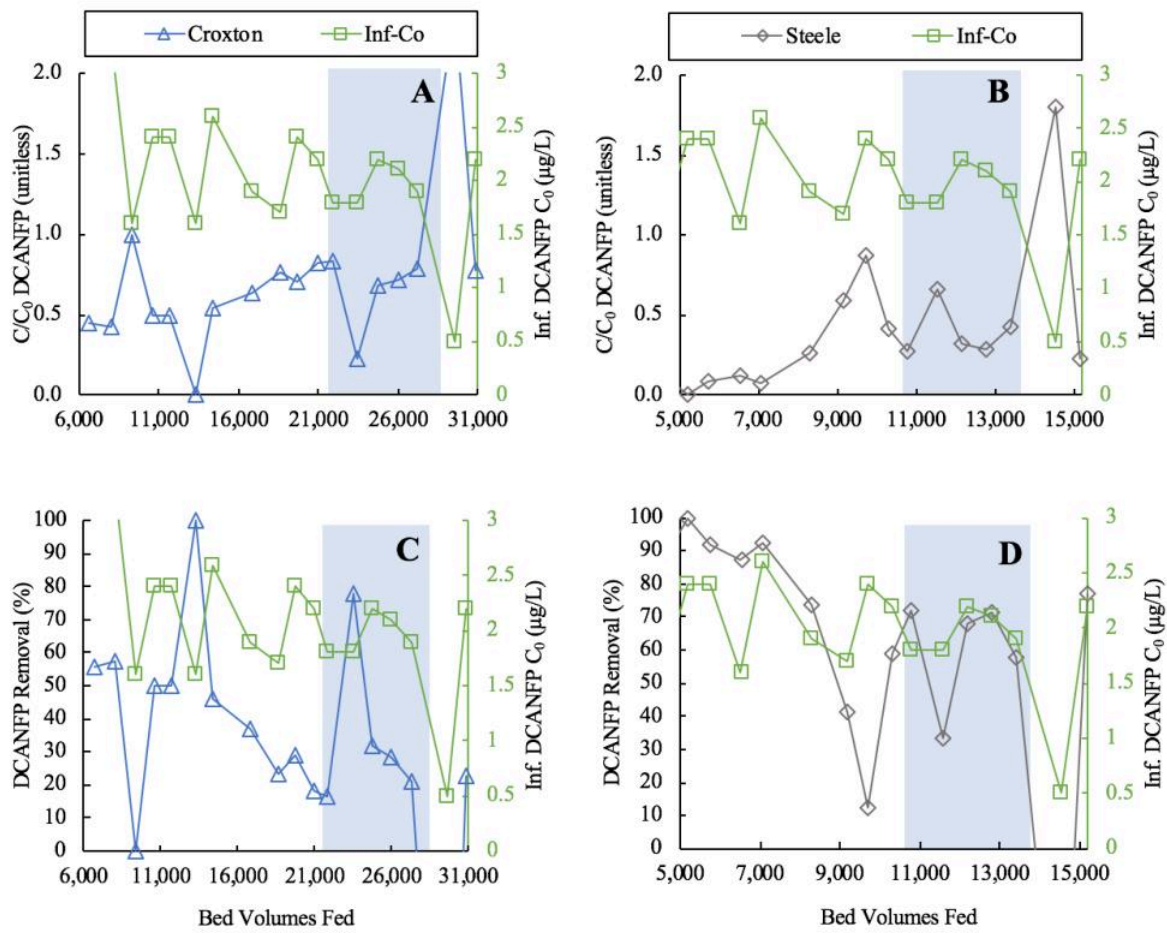


Figure 3-6. Influent-normalized (C/C_0) profiles in the Pilot filters for DCAN (A & B) and % DCANFP removal (C & D). Influent concentration (C_0) is shown on the secondary y-axis. The shaded area represents the duration for which the influent was supplemented with free ammonia at 1 mg/L-N.

3.4 Correlations between PARAFAC components

The F_{\max} values for PARAFAC components C1 and C2 for fulvic- and humic-like fluorophores respectively, are linearly dependent and strongly correlated (see Figure A-2, $R^2 = 0.90$ and 0.97 for the RSSCTs and Pilot filters, respectively). Therefore, C2 was not investigated as a DBPFP precursor surrogate. The correlation between C1 and component 3 (C3) was moderate ($R^2 = 0.63$, Figure A-2B) for the RSSCTs and strong for the Pilot filters ($R^2 = 0.95$, Figure A-2D). The stronger correlation in the Pilot filters is likely due to the predominance of physical-chemical sorption in these filters relative to the biological conditions in the RSSCTs. As C3 is a protein-like fluorophore as identified in Section 3.2, it was investigated as a DBPFP precursor surrogate.

3.5 Assessment of NOM Surrogates as DBP Precursors

Simple linear regression was used to assess the usefulness of UV_{254} , DOC and F_{\max} for C1 and C3 as surrogates of DBPFP. In the RSSCTs, the coefficient of determination values between TTHMFP and UV_{254} , DOC, C1 and C3 were low ($R^2 < 0.1$) and the slopes of these regressions were not significantly different than zero ($p > 0.05$) for each with the exception of TTHMFP- UV_{254} (see Table 3-4 and Figure A-3). However, as the R^2 value for the TTHMFP- UV_{254} is 0.07 , the prediction intervals of TTHMFP based on UV_{254} would be large and of little or no value. Similarly, between DCANFP and the precursor surrogates, the coefficient of determination values were low ($R^2 < 0.36$) and each slope was significantly different from zero ($p < 0.05$) (see Table 3-4 and Figure A-4). Higher R^2 values were observed between DBPFP and its surrogates for the pilot study (Table 3-4 and Figure A-5, $R^2 = 0.77$ between TTHMFP and C1) that are comparable to those reported in the literature ($R^2 > 0.8$) (Zheng et al. 2015). Pifer et al. (2014) reported TTHMFP to be correlated with DOC and UV_{254} ($R^2 > 0.75$) as well with humic fractions of DOC ($R^2 > 0.73$). However, that these studies were on coagulated waters in the absence of biofiltration. In case of engineered

biofiltration, particularly nitrifying biofilters, nitrate increases between the influent and effluent due to the oxidation of free ammonia. It is well known that the presence of $\text{NO}_3^-/\text{NO}_2^-$ interferes with absorbance-based measurements such as fluorescence spectroscopy and UV_{254} absorbance (Weishaar et al. 2003). Therefore, the lower R^2 values between TTHMFP and NOM surrogates may be partially due to $\text{NO}_3^-/\text{NO}_2^-$ interferences during the active period of nitrification. Fu et al. (2017) and Delatolla et al. (2015) also reported weak correlations between DBPFP and NOM surrogates for engineered biofiltration studies involving active nitrification but did not determine the underlying cause.

The RSSCT and Pilot filter data was reanalyzed following a split into two bins: (1) results prior to active nitrification (Pre-N) and (2) results during the active nitrification (Act-N) period. This produced higher R^2 values between DBPFP and the precursor surrogates for the Pre-N condition (Table 3-4). Specifically, higher coefficient of determination values were obtained for TTHMFP and C1 ($R^2 = 0.73$ and 0.76 for the RSSCTs and Pilot filters, respectively) and TTHMFP and UV_{254} ($R^2 = 0.63$ and 0.79 for the RSSCTs and Pilot filters, respectively), which are similar to previous studies (Edzwald et al. 1999, Wassink et al. 2011, Pifer et al. 2014, Zheng et al. 2015). This suggests that all four surrogates shown in Table 3-4 (UV_{254} , DOC, C1, and C3) were good predictors of TTHMFP in the absence of active nitrification in the RSSCTs and pilot filters. Importantly, the low R^2 values (< 0.27) during active nitrification in the RSSCTs indicate that the fluorescence PARAFAC components would yield large prediction intervals of TTHMFP during concomitant ammonia oxidation to nitrate.

In contrast, for Pre-N conditions in the RSSCTs, the DCANFP-C1 coefficient of determination is moderate ($R^2 = 0.66$) and higher than that for active nitrification conditions ($R^2 = 0.48$). However, the coefficient of determination between DCANFP and C3 for Pre-N ($R^2 = 0.06$ and $p > 0.05$) is

lower than that for Act-N ($R^2 = 0.58$ and $p < 0.001$). The DCANFP-C3 correlation for the pilot data also improves under active nitrification conditions ($R^2 = 0.74$ and $p < 0.001$). This suggests that DCAN precursors are captured by the protein-like C3 value which may be released during active nitrification.

Table 3-4. Coefficients of determination between DBPFP and its precursor surrogates for the overall, pre-nitrification only, and active nitrification only for the RSSCTs and Pilot filters

Correlation	RSSCTs			Pilot filters		
	Overall R^2	Pre-N R^2	Act-N R^2	Overall R^2	Pre-N R^2	Act-N R^2
TTHMFP vs. UV ₂₅₄	0.07**	0.63***	0.17**	0.61***	0.79***	0.29*
DCANFP vs. UV ₂₅₄	0.36***	0.48***	0.42***	0.54***	0.69***	0.45**
TTHMFP vs. DOC	0.003 ^{ns}	0.57***	0.01 ^{ns}	0.46***	0.69***	0.17 ^{ns}
DCANFP vs. DOC	0.05*	0.51***	0.09*	0.48***	0.66***	0.33*
TTHMFP vs. C1	0.02 ^{ns}	0.73***	0.22***	0.77***	0.76***	0.83***
DCANFP vs. C1	0.29***	0.66***	0.48***	0.72***	0.75***	0.76***
TTHMFP vs. C3	0.02 ^{ns}	0.29*	0.27***	0.72***	0.72***	0.81***
DCANFP vs. C3	0.29***	0.06 ^{ns}	0.58***	0.69***	0.69***	0.74***

^{ns} slope not significantly different than zero at $\alpha = 0.05$

* slope significantly different from zero at $p < 0.05$

** slope significantly different from at $p < 0.01$

*** slope significantly different from at $p < 0.001$

3.6 Impact of nutrient supplementation

The RSSCTs were supplemented with nutrients (free ammonia and phosphate) at a C:N:P ratio of 100:40:8 for a period of 11 weeks (7/25/18 to 10/11/18). Pilot filters were supplemented with nutrients for about 4 weeks (9/11/18 to 10/11/18). Complete oxidation of free ammonia occurred in the RSSCTs and Pilot filters which decreased the pH and increased nitrite and nitrate. The inorganic nitrogen balance for the influent and effluent water in the RSSCTs is shown in Figure 3-7.

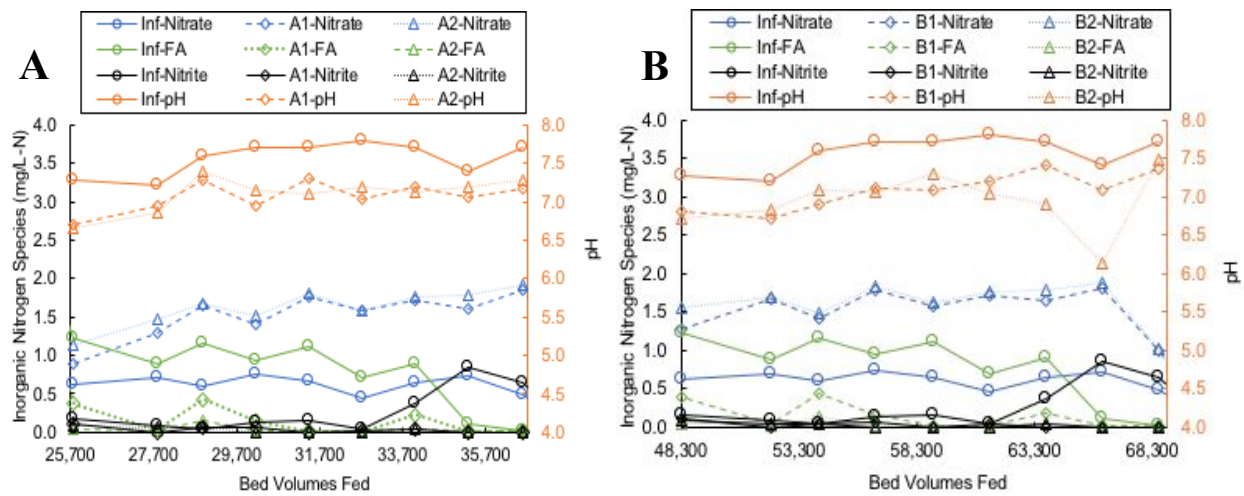


Figure 3-7. Inorganic nitrogen balance for the RSSCTs showing biological oxidation of free ammonia ($\text{NH}_4\text{-N}$) to nitrite ($\text{NO}_2\text{-N}$) and nitrate ($\text{NO}_3\text{-N}$) and the impact on pH.

In the RSSCTs, the removal of DOC, SUVA_{254} , TTHMFP, and DCANFP did not improve during the period of active nitrification (Figures 3-8). Similar results were found in Pilot filters shown in Figure 3-9. The negative SUVA_{254} removals occurred only during active nitrification period and due to the positive interference of $\text{NO}_3^-/\text{NO}_2^-$ as reported by Weishaar et al. (2003). The nutrient amendments in the RSSCTs had higher C:N:P ratio (100:40:8) than the one reported by LeChevallier et al. (1991) (100:10:1) for optimal microbial growth. Similar impact of nutrient

amendment on TTHM precursor removal was reported by (Azzeh et al. 2015) for a C:N:P ratio of 100:40:20.

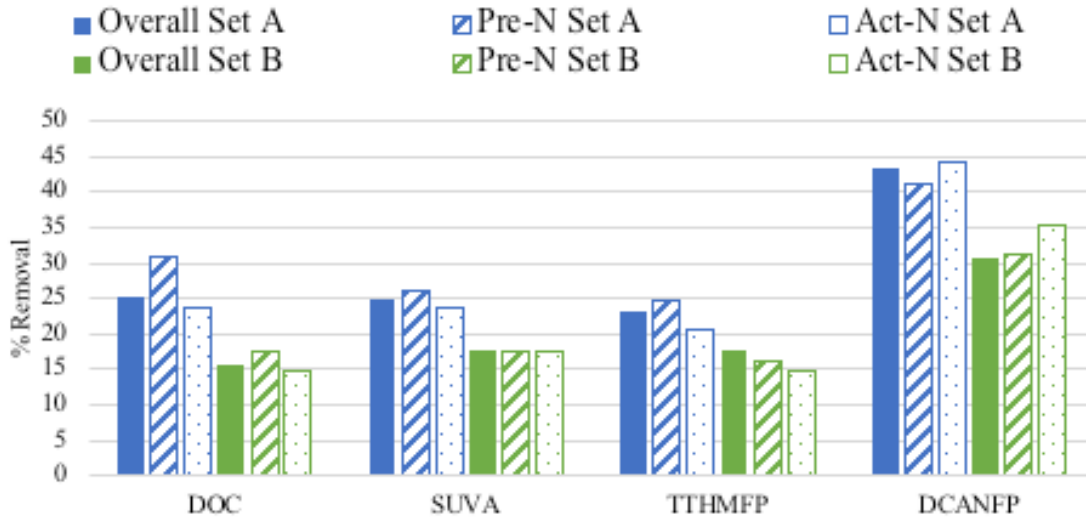


Figure 3-8. Average DOC, SUVA₂₅₄, TTHMFP and DCANFP removal for overall study period, pre-nitrification and active nitrification period in the RSSCTs.

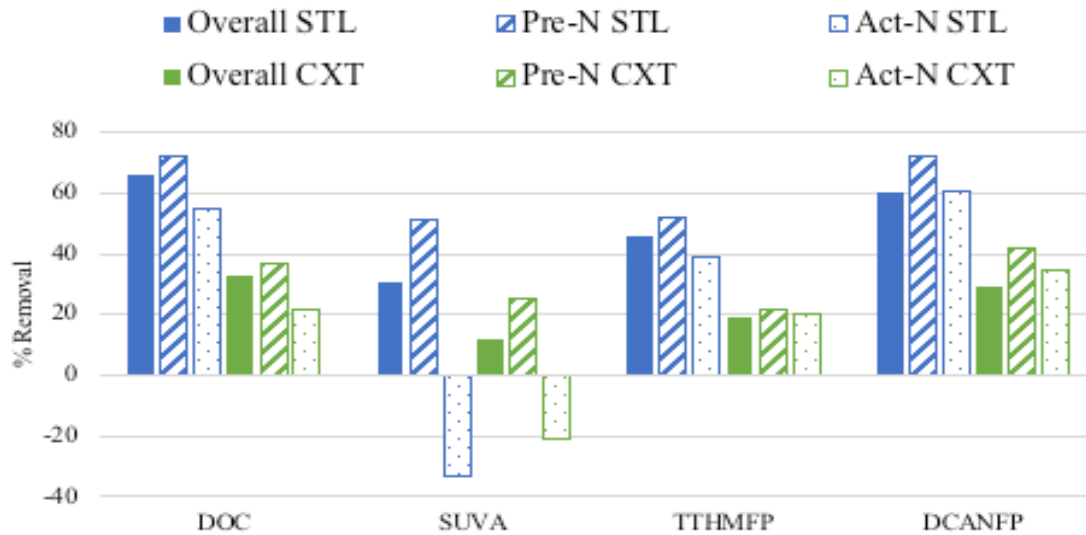


Figure 3-9. Average DOC, SUVA₂₅₄, TTHMFP and DCANFP removal for overall study period, pre-nitrification and active nitrification period in the Pilot filters (Steele and Croxton)

4 Conclusion and Future Work

The following conclusions are drawn from the RSSCTs and Pilot filters in which the extent of TTHMFP and DCANFP removal was quantified in nutrient-amended biofiltration without pre-ozonation:

- For the nitrifying RSSCTs containing GAC exhausted with respect to DOC, the average DOC removal increased ($\alpha = 0.01$) from the Influent to A1, A1 to A2, and the Influent to B2, indicating more removal with increasing EBCT between 4 and 16 mins; further, for an EBCT of 8 min (i.e., A1 and B2), there was no difference ($\alpha = 0.01$) in average DOC removals.
- In the Pilot filters, higher average DOC removal ($\alpha = 0.01$) was observed in Steele (66%) than in Croxton (33%) for EBCTs of 16 and 8 mins, respectively.
- For TTHM and DCAN precursors in the RSSCTs, there was no statistically significant removal ($\alpha = 0.01$) in B1 (EBCT = 4 mins), but removal occurred in A1 (EBCT = 8 mins) to a similar extent as A2 (EBCT = 16 mins) and B2 (EBCT = 8 mins). The lack of statistically significant ($\alpha = 0.01$) increased removal from an EBCT of 8- to 16 mins suggests that additional EBCT would not be helpful unless additional biodegradable NOM is produced using pre-ozonation or a higher chlorine dioxide dose.
- In the Pilot filters, removal of TTHMFP and DCANFP are higher in Steele (EBCT = 16 mins) compared to Croxton (EBCT = 8 mins) but these filters were removing DBP precursors by physical-chemical sorption in addition to biofiltration.
- For the period prior to active nitrification, moderate coefficients of determination were obtained for TTHMFP and C1 ($R^2 = 0.73$ and 0.76 for the RSSCTs and Pilot filters, respectively) and TTHMFP and UV_{254} ($R^2 = 0.63$ and 0.79 for the RSSCTs and Pilot filters, respectively).

- Low coefficients of determination ($R^2 < 0.27$) observed during active nitrification indicate that fluorescence PARAFAC components values would yield wide prediction intervals of TTHMFP and thus would not be useful surrogates; as a result DBPFP must be measured to assess the efficacy of biofiltration.

This study showed that biofiltration without pre-ozonation can be used to achieve removal of THM precursors in RSSCTs. Future work should focus on operation of the Pilot filters in pure biological mode following GAC exhaustion with respect to DOC and the impact of C:N:P ratio and the frequency of biofilter backwash rate on THM precursor removal. Delatolla et al. (2015) demonstrated in a pilot study that higher removal of TTHMFP and HAAFP were achieved when the filtration cycle times between backwashing events were shorter than the 7-day period used in this study. Furthermore, biofiltration performance should be evaluated by monitoring a wider range of DBPs including various unregulated DBPs such as haloacetaldehydes, haloketones, halonitromethanes and *N*-nitrosamines.

5 References

- Bull, R. J. and F. C. Kopfler (1991). Health effects of disinfectants and disinfection by-products, AWWA.
- Morris, R. D., et al. (1992). "Chlorination, chlorination by-products, and cancer: a meta-analysis." American journal of public health **82**(7): 955-963.
- Pifer, A. D. and J. L. Fairey (2012). "Improving on SUVA₂₅₄ using fluorescence-PARAFAC analysis and asymmetric flow-field flow fractionation for assessing disinfection byproduct formation and control." Water research **46**(9): 2927-2936.
- Rook, J. J. (1974). "Formation of haloforms during chlorination of natural waters." Water Treat. Exam. **23**: 234-243.
- Akcay, M. U., et al. (2016). "Effect of biofiltration process on the control of THMs and HAAs in drinking water." Desalination and Water Treatment **57**(6): 2546-2554.
- Aziz, C., et al. (1999). "Cometabolism of chlorinated solvents and binary chlorinated solvent mixtures using *M. trichosporium* OB3b PP358." Biotechnology and Bioengineering **65**(1): 100-107.
- Azzeh, J., et al. (2015). "Engineered biofiltration for ultrafiltration fouling mitigation and disinfection by-product precursor control." Water Science and Technology: Water Supply **15**(1): 124-133.
- Baghoth, S., et al. (2011). "Tracking natural organic matter (NOM) in a drinking water treatment plant using fluorescence excitation–emission matrices and PARAFAC." Water research **45**(2): 797-809.
- Basu, O. D., et al. (2016). "Applications of biofiltration in drinking water treatment—a review." Journal of Chemical Technology & Biotechnology **91**(3): 585-595.
- Benner, J., et al. (2013). "Is biological treatment a viable alternative for micropollutant removal in drinking water treatment processes?" Water research **47**(16): 5955-5976.
- Beyenal, H. and Z. Lewandowski (2002). "Internal and external mass transfer in biofilms grown at various flow velocities." Biotechnology progress **18**(1): 55-61.
- Brezonik, P. and W. Arnold (2011). Water chemistry: an introduction to the chemistry of natural and engineered aquatic systems, OUP USA.
- Brown, L. C. and P. Mac Berthouex (2002). Statistics for environmental engineers, CRC press.
- Bull, R. J. and F. C. Kopfler (1991). Health effects of disinfectants and disinfection by-products, AWWA.

Carlson, K. H. and G. L. Amy (1998). "BOM removal during biofiltration." Journal-American Water Works Association **90**(12): 42-52.

Cheremisinoff, P. N. and F. Ellerbusch (1978). Carbon adsorption handbook, Ann Arbor Science Publishers.

Chowdhury, Z. K. (2013). Activated carbon: solutions for improving water quality, American Water Works Association.

Coble, P. G. (1996). "Characterization of marine and terrestrial DOM in seawater using excitation-emission matrix spectroscopy." Marine chemistry **51**(4): 325-346.

Delatolla, R., et al. (2015). "Disinfection byproduct formation during biofiltration cycle: implications for drinking water production." Chemosphere **136**: 190-197.

Do, T. D., et al. (2015). "Improved (and singular) disinfectant protocol for indirectly assessing organic precursor concentrations of trihalomethanes and dihaloacetonitriles." Environmental science & technology **49**(16): 9858-9865.

Edzwald, J. K. and J. E. Tobiason (1999). "Enhanced coagulation: US requirements and a broader view." Water Science and Technology **40**(9): 63-70.

Fu, J., et al. (2017). "Pilot investigation of two-stage biofiltration for removal of natural organic matter in drinking water treatment." Chemosphere **166**: 311-322.

Gopal, K., et al. (2007). "Chlorination byproducts, their toxicodynamics and removal from drinking water." Journal of hazardous materials **140**(1-2): 1-6.

Kohl, P. M. and D. Dixon (2012). Occurrence, impacts, and removal of manganese in biofiltration processes, Water Research Foundation.

LeChevallier, M. W., et al. (1991). "Bacterial nutrients in drinking water." Applied and environmental microbiology **57**(3): 857-862.

Liao, X., et al. (2013). "Changes of biomass and bacterial communities in biological activated carbon filters for drinking water treatment." Process Biochemistry **48**(2): 312-316.

Liu, C., et al. (2017). "The control of disinfection byproducts and their precursors in biologically active filtration processes." Water research **124**: 630-653.

Luo, Y., et al. (2014). "A review on the occurrence of micropollutants in the aquatic environment and their fate and removal during wastewater treatment." Science of the total environment **473**: 619-641.

Morris, R. D., et al. (1992). "Chlorination, chlorination by-products, and cancer: a meta-analysis." American journal of public health **82**(7): 955-963.

Muellner, M. G., et al. (2007). "Haloacetonitriles vs. regulated haloacetic acids: are nitrogen-containing DBPs more toxic?" Environmental science & technology **41**(2): 645-651.

Nuzzo, R. (2014). "Statistical errors: P values, the gold standard of statistical validity, are not as reliable as many scientists assume." Nature **506**(7487): 150-153.

Pifer, A. D. and J. L. Fairey (2012). "Improving on SUVA₂₅₄ using fluorescence-PARAFAC analysis and asymmetric flow-field flow fractionation for assessing disinfection byproduct formation and control." Water research **46**(9): 2927-2936.

Pifer, A. D. and J. L. Fairey (2014). "Suitability of organic matter surrogates to predict trihalomethane formation in drinking water sources." Environmental engineering science **31**(3): 117-126.

Pifer, A. D., et al. (2011). "Coupling asymmetric flow-field flow fractionation and fluorescence parallel factor analysis reveals stratification of dissolved organic matter in a drinking water reservoir." Journal of Chromatography A **1218**(27): 4167-4178.

Price, M. L., et al. (1993). "Evaluation of ozone/biological treatment for disinfection byproducts control and biologically stable water."

Rice, R. G. and C. M. Robson (1982). "Biological activated carbon." Ann Arbor Sci., Ann Arbor, Mich.

Richardson, S. and C. Postigo (2012). "Drinking Water Disinfection By-products Springer Berlin/Heidelberg." City.

Richardson, S. and C. Postigo (2012). "Emerging organic contaminants and human health." The Handbook of Environmental Chemistry: 93-137.

Rook, J. J. (1974). "Formation of haloforms during chlorination of natural waters." Water Treat. Exam. **23**: 234-243.

Santín, C., et al. (2009). "Characterizing humic substances from estuarine soils and sediments by excitation-emission matrix spectroscopy and parallel factor analysis." Biogeochemistry **96**(1-3): 131-147.

Schreiber, I. M. and W. A. Mitch (2005). "Influence of the order of reagent addition on NDMA formation during chloramination." Environmental science & technology **39**(10): 3811-3818.

Selbes, M., et al. (2017). "Removal of Selected C-and N-DBP Precursors in Biologically Active Filters." Journal-American Water Works Association **109**(3): E73-E84.

Servais, P., et al. (1994). "Biological colonization of granular activated carbon filters in drinking-water treatment." Journal of Environmental Engineering **120**(4): 888-899.

Wahman, D. G., et al. (2005). "Cometabolism of trihalomethanes by *Nitrosomonas europaea*." Applied and environmental microbiology **71**(12): 7980-7986.

Wang, J. Z., et al. (1995). "Biofiltration performance: part 1, relationship to biomass." Journal-American Water Works Association **87**(12): 55-63.

Wassink, J., et al. (2011). "Evaluation of fluorescence excitation–emission and LC-OCD as methods of detecting removal of NOM and DBP precursors by enhanced coagulation." Water Science and Technology: Water Supply **11**(5): 621-630.

Weishaar, J. L., et al. (2003). "Evaluation of specific ultraviolet absorbance as an indicator of the chemical composition and reactivity of dissolved organic carbon." Environmental science & technology **37**(20): 4702-4708.

Zearley, T. L. and R. S. Summers (2012). "Removal of trace organic micropollutants by drinking water biological filters." Environmental science & technology **46**(17): 9412-9419.

Zepp, R. G., et al. (2004). "Dissolved organic fluorophores in southeastern US coastal waters: correction method for eliminating Rayleigh and Raman scattering peaks in excitation–emission matrices." Marine chemistry **89**(1-4): 15-36.

Zheng, D., et al. (2015). "Effects of coagulation on the removal of natural organic matter, genotoxicity, and precursors to halogenated furanones." Water research **70**: 118-129.

Zhu, I. X., et al. (2010). "Review of biologically active filters in drinking water applications." Journal-American Water Works Association **102**(12): 67-77.

6 Appendix

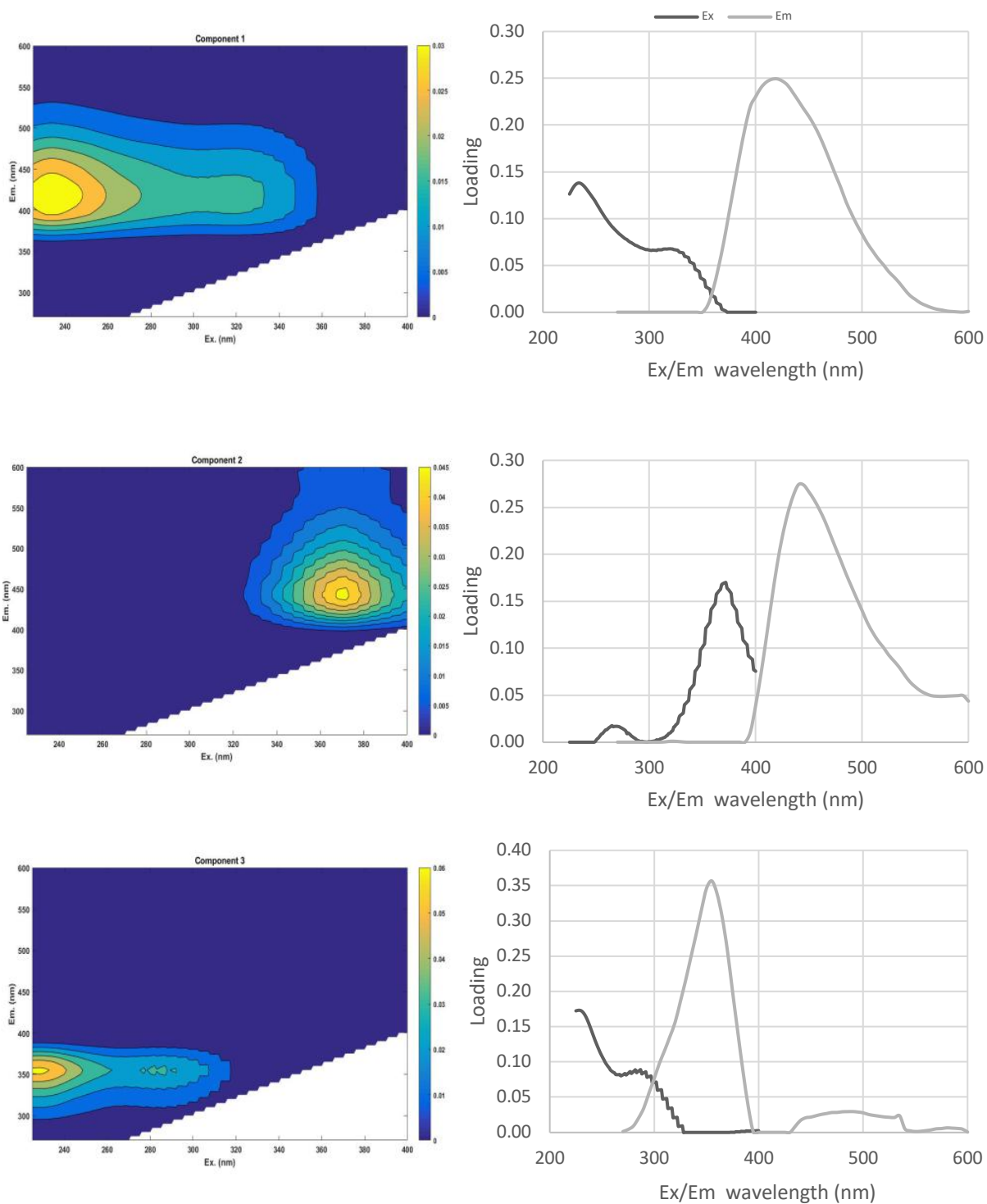


Figure A-1. Contour plots and excitation emission loadings of fluorescence components 1, 2 and 3 obtained from PARAFAC analysis of 426 EEMs

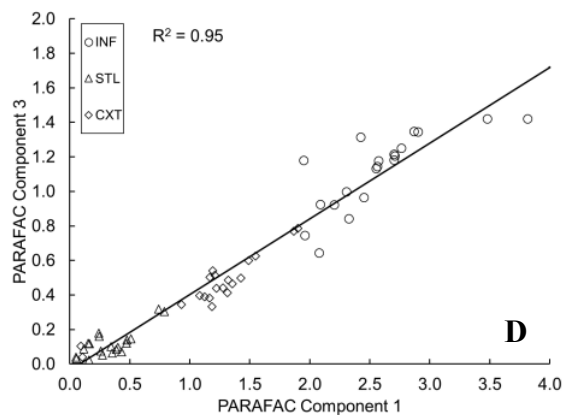
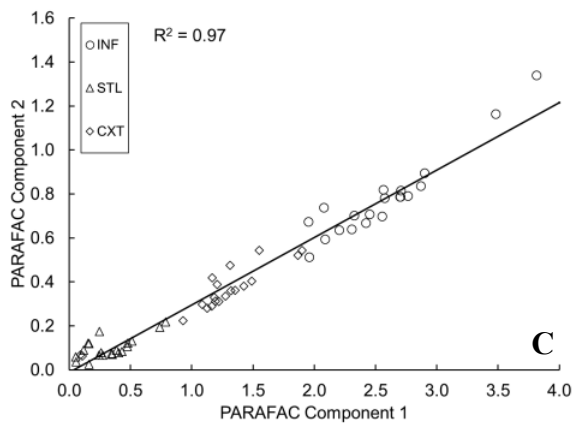
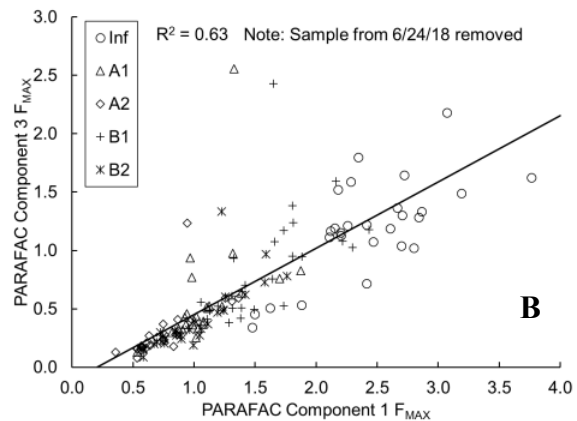
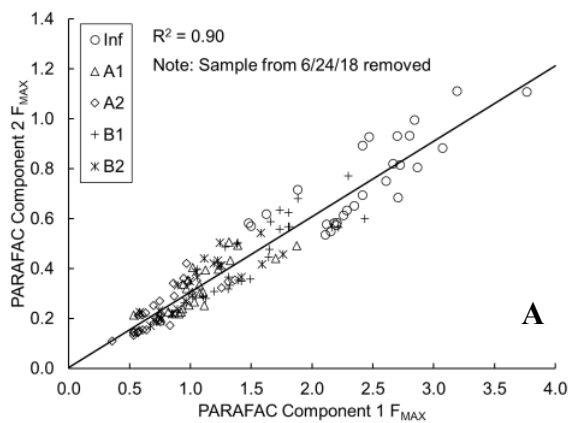


Figure A-2. Correlations between PARAFAC components (C1 & C2) and (C1 & C3) for RSSCTs (A & B) and pilot filters (C & D).

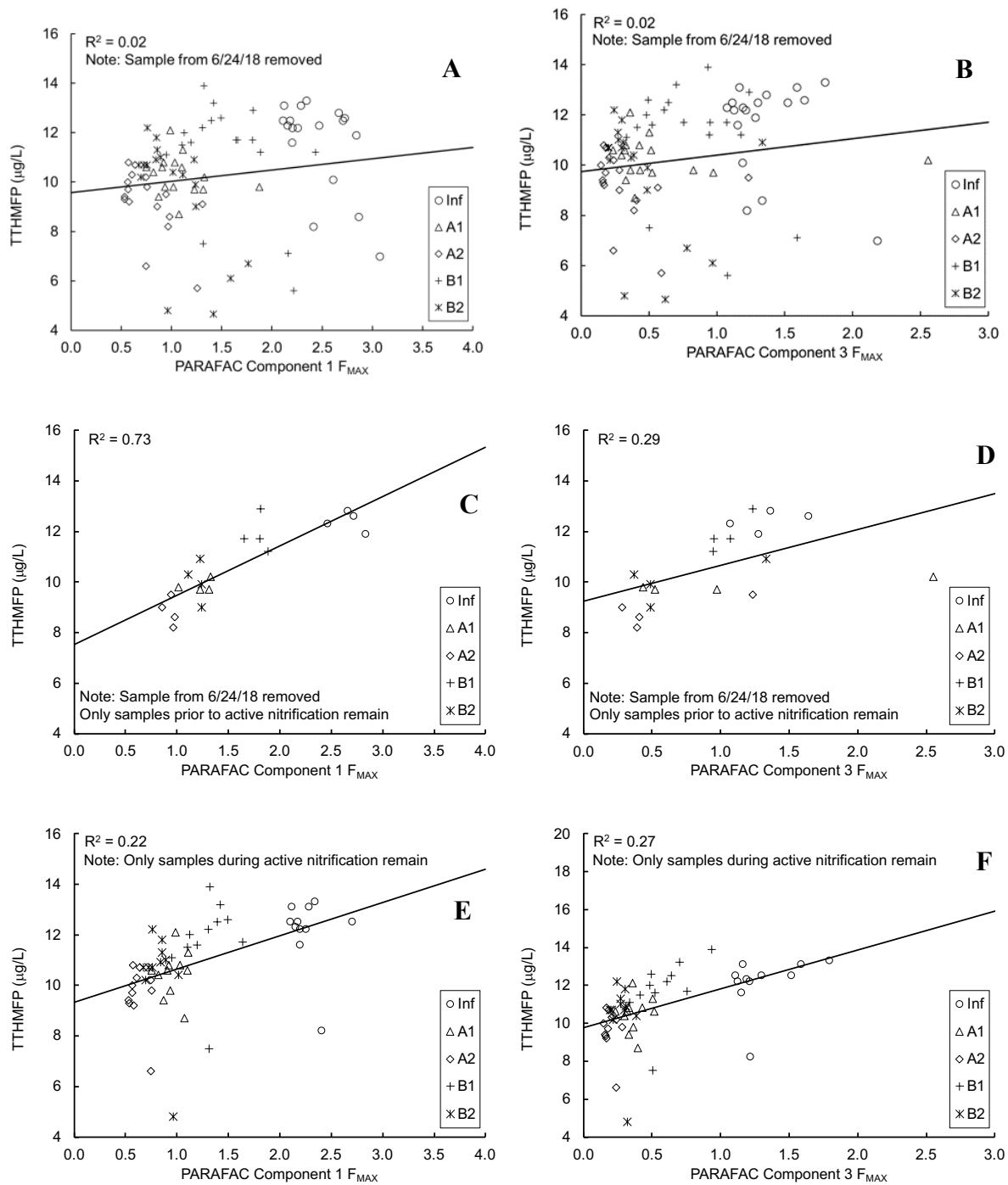


Figure A-3. Correlations between TTHMFP and PARAFAC components C1 and C3 for overall (A & B), pre-nitrification (C & D) and active-nitrification period (E & F) in RSSCT.

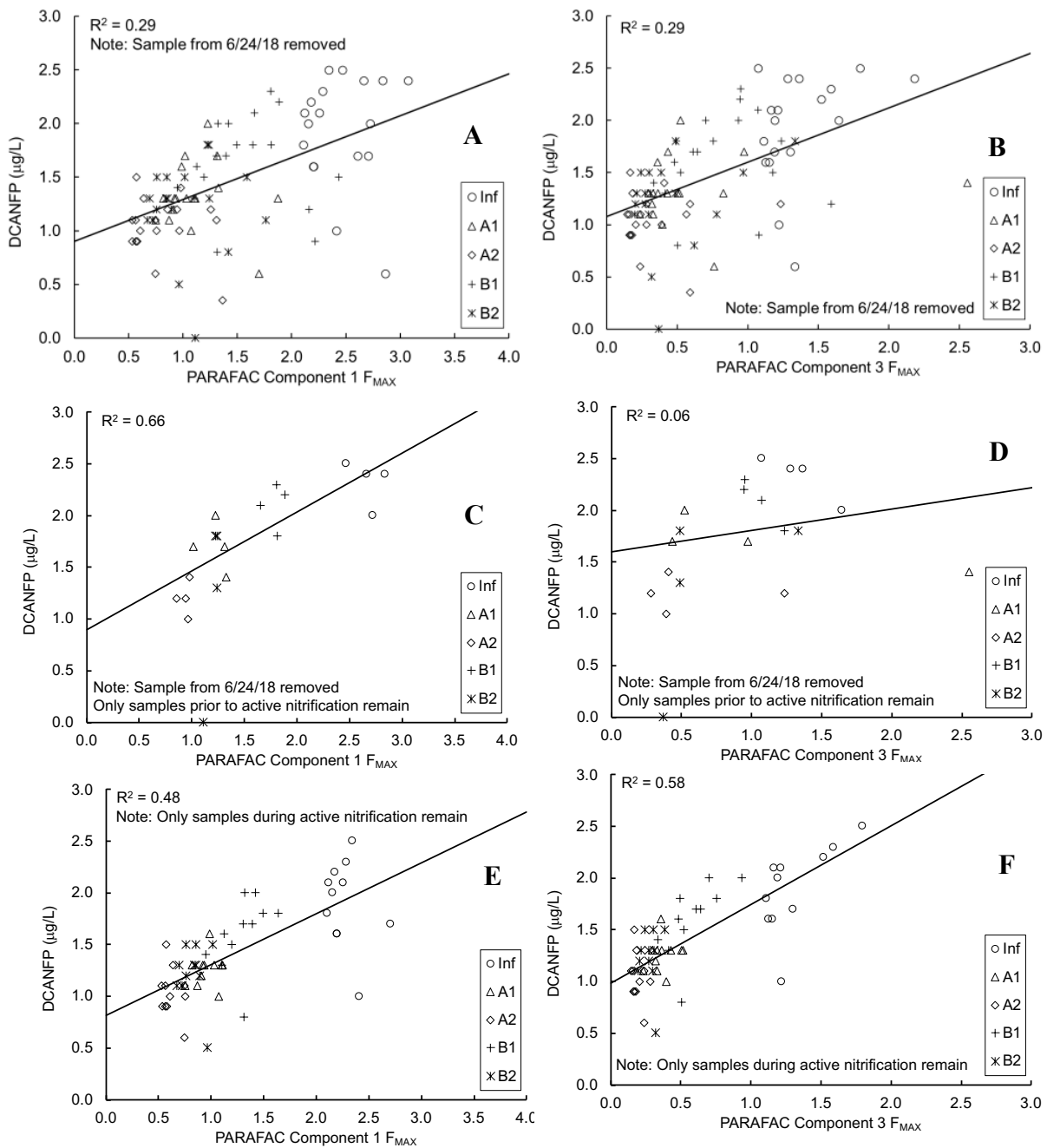


Figure A-4. Correlations between DCANFP and PARAFAC components C1 and C3 for overall (A & B), pre-nitrification (C & D) and active-nitrification period (E & F) in RSSCT.

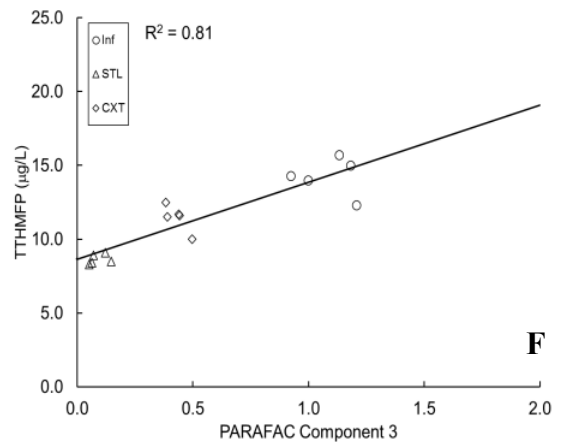
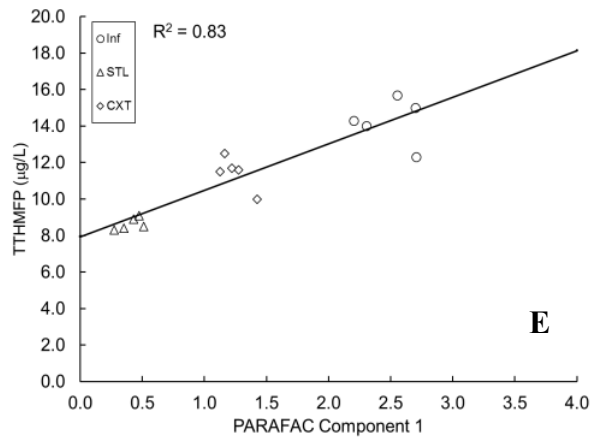
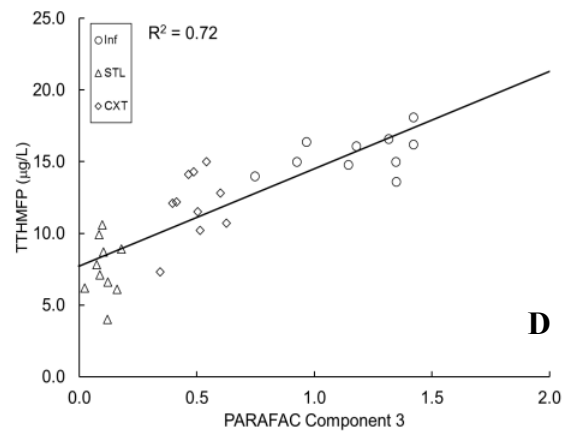
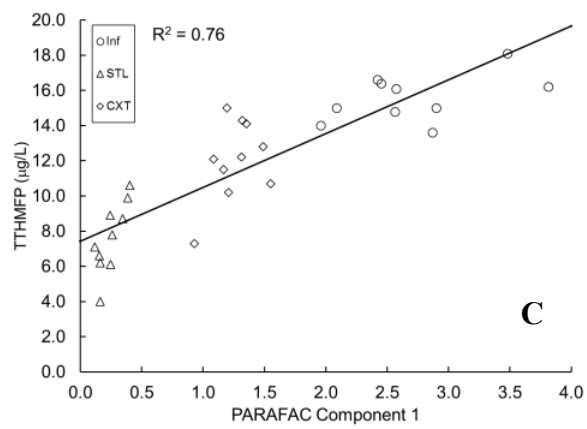
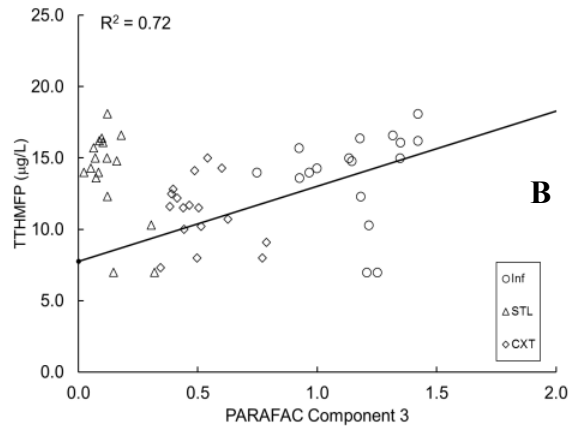
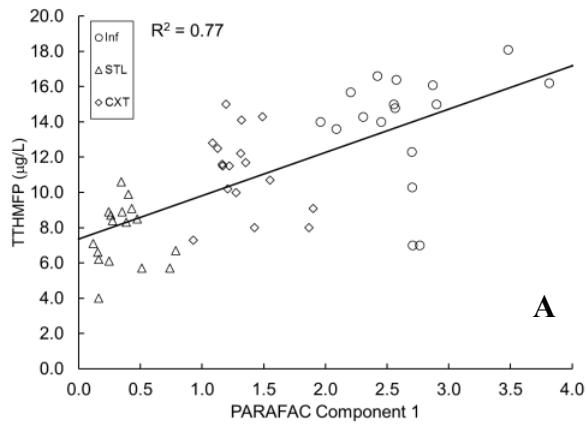


Figure A-5. Correlations between TTHMFP and PARAFAC components C1 and C3 for overall (A & B), pre-nitrification (C & D) and active-nitrification period (E & F) in pilot filters.

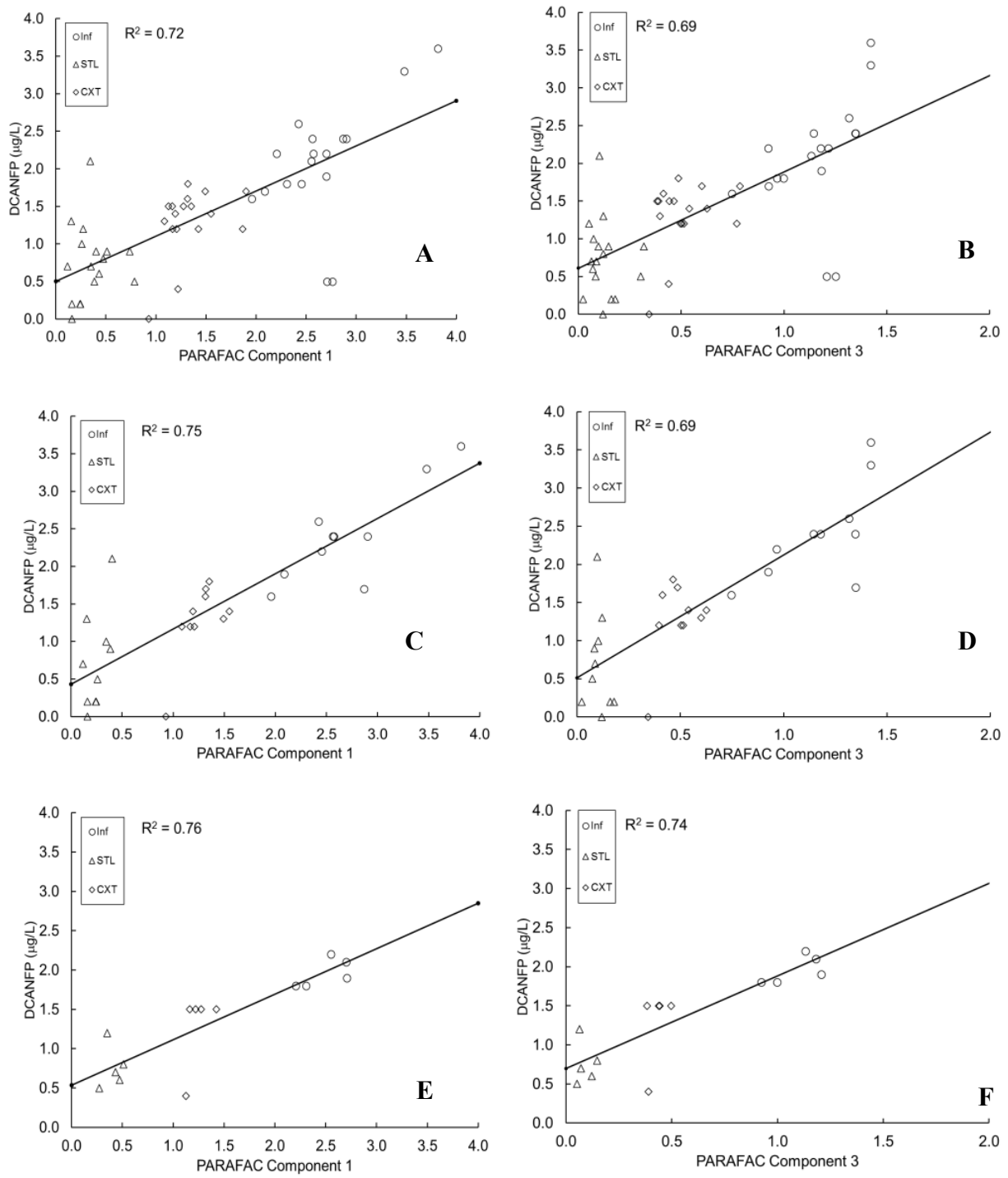


Figure A-6. Correlations between DCANFP and PARAFAC components C1 and C3 for overall (A & B), pre-nitrification (C & D) and active-nitrification period (E & F) in pilot filters.